# NF45/NF90-mediated rDNA transcription provides a novel target for immunosuppressant development

Hsiang-i Tsai[1,*], Xiaobin Zeng[2,*], Longshan Liu[3,*], Shengchang Xin[4], Yingyi Wu[1], Zhanxue Xu[1], Gan Liu[1], Zirong Bi[3], Dandan Su[1], Min Yang[1], Changxi Wang[3], Jing Zhao[4], John E. Eriksson[5], Wenbin Deng[1#], Fang Cheng[1,#], Hongbo Chen[1,#]

1. School of Pharmaceutical Sciences (Shenzhen), Sun Yat-Sen University, Shenzhen 518107, PR China.
2. Center Lab of Longhua Branch and Department of Infectious Disease, Shenzhen People's Hospital, 2nd Clinical Medical College of Jinan University, and Guangdong Provincial Key Laboratory of Regional Immunity and Diseases, Medicine School of Shenzhen University, Shenzhen 518037, Guangdong Province, China.
3. Organ Transplant Center，The First Affiliated Hospital, Sun Yat-sen University, 58 Zhongshan 2nd Road, Guangzhou, Guangdong 510080, China.
4. State Key Laboratory of Coordination Chemistry, Institute of Chemistry and Biomedical Sciences, School of Life Sciences, Nanjing University, Nanjing 210023, China.
5. Cell Biology, Biosciences, Faculty of Science and Engineering, Åbo Akademi University, FI-20520, Turku, Finland; Turku Centre for Biotechnology, University of Turku and Åbo Akademi University, FI-20521, Turku, Finland.

***** These authors contributed equally to this work

#To whom correspondence may be addressed: dengwb5@mail.sysu.edu.cn (Wenbin Deng), Chengf9@mail.sysu.edu.cn (Fang Cheng), chenhb7@mail.sysu.edu.cn (Hongbo Chen).

# Abstract

Herein, we demonstrate that NFAT, a key regulator of the immune response, translocates from cytoplasm to nucleolus and interacts with NF45/NF90 complex to collaboratively promote rDNA transcription via triggering the directly binding of NF45/NF90 to the ARRE2 consensus sequences in rDNA promoter upon T cell activation *in vitro*. The elevated pre-rRNA level of T cells are also observed in both mouse heart or skin transplantation models, and in kidney transplanted patients. Importantly, T cell activation can be significantly suppressed by inhibiting NF45/NF90-dependent rDNA transcription. Amazingly, CX5461, a rDNA transcription specific inhibitor, outperformed FK506, the most commonly used immunosuppressant, both in terms of potency and off-target activity (i.e. toxicity), as demonstrated by a series of skin and heart allograft models. Collectively, this reveals NF45/NF90-mediated rDNA transcription as a novel signaling pathway essential for T cell activation, and as a new target for the development of safe and effective immunosuppressants.


**Keyword:** NF45/NF90; immunosuppressive agents; organ transplant rejection; calcineurin-NFAT pathway; nucleolus

# Introduction

The inhibition of T cell activation is crucial for both the prevention of organ transplantation rejection and graft-versus-host disease (GVHD) that accompanies allogeneic hematopoietic stem cell transplantation, as well as in the treatment of certain autoimmune diseases (Skeens et al, 2019). The calcineurin–NFAT (nuclear factor of activated T cells) binding inhibitors cyclosporine A (CsA) and tacrolimus (FK506) have proven highly effective at suppressing T cell response to allografts, and are among the most widely used immunosuppressive drugs to significantly prolong graft survival and reduce patient morbidity (Monostory, 2018). The use of these immunosuppressive agents has also been reported in a variety of autoimmune diseases (Borroto et al, 2016). Despite their widespread application in the clinic, calcineurin inhibitors have been the cause of myriad side effects, including nephrotoxicity, chronic kidney damage, and post-transplant malignancies (Group et al, 2018). This may be the result of the general inhibition of calcineurin activity, which plays other biologically important roles besides NFAT activation. The discovery of novel mechanisms of early T cell activation that obviate the inhibition of calcineurin is therefore of great value in the search for safer and more efficient immunosuppressive agents.

The $Ca^{2+}$-calcineurin-NFAT signaling pathway is a master regulator of T cell proliferation and activation (Okeefe et al, 1992). During an adaptive immune response, phosphatase calcineurin dephosphorylates NFAT1 (also known as NFATc2) and NFAT2 (also known as NFATc1) within T cells. The dephosphorylated NFAT1 and NFAT2 then translocate from the cytoplasm to the nucleus, where they bind directly to antigen response recognition element 2 (AARE2) within the interleukin-2 (IL-2) enhancer region. This in turn induces IL-2 gene transcription (Jain et al, 1993), an essential cytokine for the clonal proliferation and activation of T lymphocytes(Broere & van Eden, 2019). The calcineurin inhibitors CsA and FK506 prevent the calcineurin-driven dephosphorylation of NFAT, thereby inhibiting NFAT nuclear accumulation, IL-2 expression, and the downstream functions of effector T cells.

The nuclear factors NF45 and NF90 were originally isolated in activated Jurkat cells as a heterodimeric complex (NF45/NF90) binding specifically to the ARRE2 enhancer element of the IL-2 promoter (Kao et al, 1994). Both NF45 and NF90 have an N-terminal "domain associated with zinc fingers" (DZF) that resembles template-free nucleotidyltransferases, and mediates the heterodimerization of NF45/NF90 through a structurally conserved interface (Wolkowicz & Cook, 2012). Moreover, NF90 has one nuclear localization signal (NLS) domain and two double-stranded RNA binding domains (dsRBDs) in the C-terminal region (Barber, 2009), which confer binding to highly structured RNAs (Parker et al, 2001). In mammals, the NF45/NF90 protein complex is expressed in a wide variety of tissues (Zhao et al, 2005), and participates in numerous cellular functions (Shim et al, 2002), including cell cycle regulation (Guan et al, 2008), transcription activation (Kiesler et al, 2010), translational control (Castella et al, 2015), DNA damage response (Shamanna et al, 2011), microRNA (miRNA) biogenesis (Masuda et al, 2013), and viral infection (Idda et al, 2019). However, the specific role of NF45/NF90 in the regulation of T cell activation has not been well established.

In this study, a novel mechanism for the regulation of rDNA transcription in the nucleolus is presented, in which the NF45/NF90 complex plays a key role by interacting with the upstream binding factor (UBF) and promoting the recruitment of RNA Pol I to rDNA promoter regions. We found that the NF45/NF90-regulation of rRNA transcription positively regulates T cell activation. Suppressing rDNA transcription using the Pol I inhibitor CX5461 significantly inhibited IL-2 secretion, reduced the proliferation of T lymphocytes, and enhanced the survival of mouse skin and heart allografts. This mechanism constitutes a novel therapeutic strategy for immunosuppression.

## Materials and Methods

### Clinical sample of kidney transplant patients

Approximately 20 mL of heparinized peripheral blood was obtained after allograft

transplantation from patients in varying groups: seven stable, eight with ABMR, and eight with TCMR. All patients gave informed consent for this study, and the study was approved by the Organ Transplant Center at the First Affiliated Hospital of Sun Yat-sen University (ClinicalTrials.gov NO.2019-456).

**Cell lines, Plasmids, siRNAs, antibodies, chemicals and dyes**

HEK293, HEK293T, Jurkat and HeLa cells were purchased from American Type Culture Collection (ATCC). Cells were cultured in RPMI 1640 or DMEM supplemented with 10% fetal calf serum (Hyclone, Logan, UT, USA), 100 units/mL penicillin, and 100 μg/mL streptomycin, and were incubated at 37 °C in a 5% $CO_2$ atmosphere. Human NF45 was cloned into the pFLAG-CMV2 vector (Sigma–Aldrich, St. Louis, MO). The pHrD-IRES-Luc plasmid contains the promoter sequence of the rDNA gene was kindly provided by Professors Ke Y and Jacob ST (Genetics Laboratory, Peking University School of Oncology, Beijing Cancer Hospital & Institute, Beijing, China) (Peng et al, 2010).

The pcDNA3.1-NF90-Flag, NF90-385-388A, NF90-432/555A, NF90-T188/T315A, NF90 (1–369 aa) and NF90 (370 aa-c) truncation plasmids were kindly gifted from Professor Honglin Chen (State Key Laboratory for Emerging Infectious Diseases, Department of Microbiology, The University of Hong Kong, Hong Kong). Chemically synthesized siRNAs specifically targeting human NF45 and NF90 were purchased from GenePharma (Shanghai, China) with the following sequences:

NF45-siRNA1: 5'-AACGAAACUGGCUUUGAAATT-3';

NF45-siRNA2: 5'- GCUGCACUUGGACAUCAAATT-3'

NF90-siRNA1: 5'-GCCCACCUUUGCUUUUUAUTT-3'

NF90-siRNA2: 5'-CAGCGUUGUUCGGCAUCAATT-3'.

The primary antibodies for p-UBF (ser 388), RPA194, nucleolin, UBF, NF45 and NF90 were purchased from Santa Cruz Biotechnology (Santa Cruz, CA, USA). The primary antibody for UBF was obtained from Abcam (Abcam, Cambridge, UK). The primary

antibodies for FLAG, anti-bromodeoxyuridine (BrdU) and GAPDH were obtained from Abmart (Abmart, Shanghai, China). HRP- and fluorescein-labeled secondary antibodies and the ECL detection system were purchased from KPL (Gaithersburg, MD, USA). Anti-FLAG M2 affinity gels (Abmart, Shanghai, China) were used to precipitate FLAG-fused proteins. Dynabeads Protein G magnetic beads used in ChIP assays were purchased from Life Technologies (Carlsbad, CA, USA). CX5461 was purchased from MCE (MedChem express, USA). FK506 was purchased from Selleck Chemicals (Shanghai, China). IL-2 was purchased from Peprotech (Rocky Hill, NJ, USA).

**Western Blotting**

Protein fractions were separated by SDS-PAGE, and then transferred to PVDF membranes. Membranes were blocked with 5% non-fat milk for 1 h at room temperature and incubated with the desired primary antibodies overnight at 4 °C. After 1 h incubation at room temperature with HRP-coupled secondary antibodies, the specific proteins were detected by using an ECL reagent.

**Nucleolus Fractionation**

Nucleoli were isolated from HEK293 cells as described previously(Hacot et al, 2010). The nuclear and nucleolar fractions were subjected to western blotting using the antibodies indicated.

**Quantitative PCR**

Total RNA was extracted using the TRIZOl regent (Invitrogen Corp., Carlsbad, CA, USA) according to the manufacturer's specification. The cDNA was synthesized by reverse transcription using random primers and the product was used to analyze mRNA using SYBR Green real-time quantitative PCR (qPCR) (Biotool, China). qPCR primers are listed in the below.

| Gene | Forward primer sequence 5'→3' | Reverse primer sequence 5'→3' |
|---|---|---|
| Human β-actin | **GAACGGTGGTGTGTCGTTC** | **GCGTCTCGTCTCGTCTCACT** |
| Human pre-rRNA | **GAACGGTGGTGTGTCGTTC** | **GCGTCTCGTCTCGTCACT** |

| | | |
|---|---|---|
| Human IL-2 | **ATTACAAGAATCCCAAACTC** | **ATTGCTGATTAAGTCCCT** |
| Mouse β-actin | **GGCTGTATTCCCCTCCATCG** | **CCAGTTGGTAACAATGCCATGT** |
| Mouse TNFα | **TCTCATCAGTTCTATGGCCC** | **GGGAGTAGACAAGGTACAAC** |
| Mouse granzyme B | **TCGACCCTACATGGCCTTAC** | **TGGGGAATGCATTTTACCAT** |
| Mouse IL-12 | **CAGCATGTGTCAATCAGCTAC** | **TGTGGTCTTCAGCAGGTTTC** |
| Mouse pre-rRNA | **CTCCTGTCTGTGGTGTCCAA** | **GCTGGCAGAACGAGAAGAAC** |

**Luciferase Reporter Assay**

HEK293T cells were first grown on 12-well plates, and then transfected with the indicated siRNAs for 48 h, followed by the addition of 1μg pHrD-IRES-Luc into the media. After a further 24 h, cells were harvested in the passive lysis buffer, and the relative rDNA promoter activity was measured in cell lysates using a dual luciferase assay kit (Promega, Madison, WI, USA).

**Immunofluorescence Assay**

Cells growing on glass coverslips were fixed and permeabilized and then blocked. After incubation with primary antibodies at 4 °C overnight, the coverslips were incubated with fluorescein or rhodamine-conjugated secondary antibodies for 1h at room temperature. Nuclei were counterstained with DAPI and imaged using a confocal microscope.

**5-Fluorouridine (Furd) Incorporation Assay**

NF45-specific, NF90-specific or control siRNAs were used to transfect HeLa cells grown on coverslips in a 12-well culture plate. FUrd (Sigma–Aldrich, St. Louis, MO, USA) was added 24 h after transfection at a final concentration of 10 mM. After 15 min. incubation, cells were subjected to immunodetection with a BrdU antibodies.

**Co-immunoprecipitation Assay (Co-IP)**

Cells were lysed in an RIPA buffer (150 mM NaCl, 0.1 % Triton X-100, 0.5% sodium deoxycholate, 0.1% SDS, 50 mM Tris-HCl, pH 8.0, nuclease, protease inhibitor cocktail) and subjected to sonication for 10 sec. The cell lysates were clarified using centrifugation at 12,000 rpm for 15 min. Protein extracts were then mixed with the

indicated primary antibodies and protein A/G agarose (Sigma, St. Louis, MO, USA) or anti-FLAG M2 agarose for overnight at 4 °C. The complexes were collected and washed three times with TBST (1X Tris-Buffered Saline, 0.1% Tween® 20 Detergent). The resolved proteins were analyzed using western blotting.

**Chromatin Immunoprecipitation (ChIP)**

ChIP was performed in an accordance with a published protocol (Nelson et al, 2006) with minor modifications. Briefly, cells were fixed with 1% formaldehyde for 15 min. at room temperature, and cross-linking reactions were then quenched by adding 125 mM glycine for 5 min. Cells were collected and resuspended in a ChIP lysis buffer (50 mM Tris-HCl pH 7.5, 150 mM NaCl, 5 mM Ethylenediaminetetraacetic acid (EDTA), 0.5% NP-40, 1.0% Triton-X-100, and protease inhibitor cocktail), then subjected to sonication to produce 200-1000 bp DNA fragments. Sheared chromatin was immunoprecipitated with the indicated antibodies or control IgG in combination with Dynabeads Protein G magnetic beads. After several washes, the beads were resuspended with Chelex 100 suspension and boiled for 10 min. Then, samples were incubated using RNase A (10 mg/mL) while shaking at 65 °C overnight. Proteinase K was added the next day and incubated in a shaker (1 h, 55 °C at 1,400 rpm) followed by boiling for 10 min. After centrifugation, the suspension was collected to perform qPCR analysis, and fold enrichment relative to the IgG control antibody was calculated. Primers (H0, H13, H23, H42.9) for the rDNA loci used in the ChIP assays were synthesized as specified previously (Grandori et al, 2005).

**Electrophoretic Mobility Shift Assays (EMSA)**

Nuclear extracts were prepared according to the protocol of Preparing Nuclear and Cytoplasmic Extracts(Lahiri & Ge, 2000). NF45/NF90 binding activity was assessed by EMSA by using an rDNA probe. Non-radioactive EMSA was performed by using EMSA/Gel-Shift kit (Beyotime Biotechnology, Shanghai, and China), the sequences of the rDNA promoter-containing oligonucleotide were as follows: F.p5′-TGGAGACACGGGCCGGCCCCCT-3′.

R.p: 5′-CAGGTCGCCAGAGGACAGCGTGTC-3′.

EMSA was carried out according to the enclosed EMSA/Gel-Shift kit protocol (Beyotime Biotechnology). Supershift assays were performed in HEK293 cells with antibodies specific for NF-45 and NF-90. The details are described in Materials and Methods section. The following controls were used. 1) Biotin – rDNA promoter. 2) Biotin – rDNA promoter + Nuclear extract. 3) Biotin – rDNA promoter + Nuclear extract + 100-fold molar excess of unlabeled rDNA promoter. 4) Biotin – rDNA promoter + Nuclear extract + 100-fold molar excess of unlabeled rDNA mutant promoter. 5) Biotin – rDNA promoter + Nuclear extract + NF90 antibody. 6) Biotin – rDNA promoter + Nuclear extract + NF45 antibody. Following 15 min. incubation at room temperature, the reactions were transferred into a pre-run 6% native polyacrylamide mini-gel and submitted to gel electrophoresis. Following electrophoretic separation, oligonucleotide-protein complexes were transferred by electro-blotting (330 mA, 1 h) onto specific positively charged nylon membranes (Bio-Rad) and detected using an anti-digoxigenin antibody conjugated with alkaline phosphatase, then revealed by autoradiography upon application of a specific luminescent substrate (Beyotime Biotechnology, Shanghai, china). The generated chemiluminescent signals were recorded on X-ray films.

**Isolation of PBMC and CD3$^+$ T cells**

Peripheral blood from normal, healthy donors was collected into potassium EDTA vacates. PBMCs were isolated using Ficoll® lymphocyte separation medium (LSM, MP Biomedicals, Aurora, USA) centrifugation as described previously (Chikamatsu et al, 2007). Cells were cultured in R10 medium (RPMI supplemented with 10% FBS, L-glutamine, penicillin/streptomycin and 10 ng/mL IL-2). Next, CD3 T cells were separated from PBMCs by using a MojoSort$^{TM}$ Human CD3$^+$ T cell Isolation Kit (Biolegend, USA). In brief, PBMCs were incubated with a biotin-antibody cocktail followed by magnetic Streptavidin Nanobeads to obtain untargeted T cells. The untargeted CD3$^+$ T cells were poured and collected the liquid. The CD3$^+$ T cells were stimulated with plate-bound anti-CD3 (OKT-3; Biolegend, USA) and anti-CD28

(Biolegend, USA) antibodies and 20 ng/mL recombinant human interleukin-2 (IL-2, Peprotech) in an RPMI1640 medium.

**Lentiviral shRNA Production, and Infection**

For constructs expressing shRNA against NF45 and NF90, in order to produce the shRNA lentivirus, the recombinant packaging plasmids were cotransfected with NF45 or NF90 plasmids into HEK 293T cells, and culture supernatants containing the virus were collected 12 h and 36 h after transfection. For infection with lentivirus, PBMC and Jurkat cells were cultured with lentiviral solution for 24 h in the presence of 1 μg/mL Polybrene (Sigma).

**CCK-8 Assay**

Cell proliferation was evaluated using the Cell Counting Kit-8 (CCK-8; Beyotime Institute of Biotechnology) and following the manufacturer's instructions. Briefly, cells were plated in 96-well plates in medium containing 10% FBS at approximately $5\times10^3$ cells/well. Then 10 μL CCK-8 solution was added to each well and incubated for 2 h. The absorbance at 450 nm was measured using a microplate reader. Results are representative of three individual experiments in triplicate.

**CFSE Staining**

Cells were labeled using CFSE working solution (5 μM) using the CFSE division tracker kit (Biolegend, USA). T cells were incubated for 20 min. at 37 ℃ and quenched staining with culture medium. Next, cells were seeded in 24 wells and re-stimulated with 2 μg $mL^{-1}$ plate-bound anti-CD3 (OKT3; Biolegend) and 2 μg $mL^{-1}$ anti-CD28 (Biolegend, USA). At days 0, 3 and 7, T cells were collected and subjected to FACS (Beckman Coulter, Brea, CA, USA) using the Cell Quest software (BD Biosciences, Mountain View, CA, USA).

**Skin Allograft and Heart Transplantation Models**

Male BALB/c mice were obtained from the Institute of Laboratory Animal Sciences,

Chinese Academy of Medical Science. All animal studies were carried out according to the protocols approved by the Administrative Committee on Animal Research of Sun Yat-sen University. The approved numbers were 2019000349 and 2019000352. All mice were maintained in a pathogen-free environment at 21 ± 2 °C and 20% humidity with a 12 h light/dark cycle. The animals were acclimatized for one week prior to use. All experiments were performed under laminar flow hoods. C56BL/6 skin transplantation was performed in eight-week-old male BALB/c mice according to a standard procedure. Skin grafts (1 $cm^2$ in size) from C56BL/6 mice were dorsally transplanted onto recipient BALB/c mice. All 48 recipients were randomly divided into four equal groups: control group (DMSO, n = 10), group 2 (CX5461 0.5 mg/kg/d, n = 10), group 3 (CX5461 1.0 mg/kg/d, n = 10), group 4 (CX5461 2.0 mg/kg/d, n = 10), group 5 (FK506 2.0 mg/kg/d, n = 10). Three days prior to skin transplantation, the recipients were treated with medicines *via* intraperitoneal injection every day until 12 days after transplantation. The allografts were observed and photographed daily for 30 days, in which the necrosis mice were calculated, where >90% necrosis of the skin allograft was defined as rejection. Graft necrosis was grossly determined based on graft appearance, color, texture, and absence of bleeding when cut with a scalpel. The mean survival time (MST) of skin grafts in all groups was calculated.

To carry out heart transplantation, hearts from male BALB/c mice as donors were transplanted into the cervices of male C57BL/6 mice (8-10 weeks old, weight >22 g). The doses and injection time of all 30 recipients were randomly divided into four equal groups: control group (DMSO, n = 10), group 2 (CX5461 2.0 mg/kg/d, n = 10), group 3 (FK506 2.0 mg/kg/d, n = 10). Three days prior to heart transplantation, the recipients were treated with medicines *via* intraperitoneal injection every day until 80 days after transplantation. Transplanted mice were sacrificed at seven days to dissect graft-heart, lymph nodes and spleen followed by downstream analysis.

**ELISA Detection of Cytokines**

The purified mice serum or PBMC cells ($10^6$ cells $mL^{-1}$) were treated with P/I, FK506

and CX5461. Their supernatants were harvested, and the concentrations of IL-2, IL-12 and IFN-γ were determined using an ELISA kit (Dakewe Biotech Inc., Co. Ltd., Shenzhen, China), by using recombinant cytokines to establish standard curves.

**Histological and Immunohistochemistry Analysis**

Seven days after surgery, the mouse recipients were sacrificed and tissue specimens from the transplantation site were collected, fixed with 4% paraformaldehyde for 24 h and embedded with paraffin. Sections (4 μm thickness) were stained with hematoxylin–eosin for conventional morphological evaluation. Ten visual fields of each sample were randomly selected to observe the inflammatory cell infiltration. For the immunohistochemical staining, deparaffinized tissue sections were incubated with mouse monoclonal CD3 (PC3/188A: sc-20047, Santa Cruz Biotechnology), followed by visualization using HRP/DAB detection IHC Kit and counterstaining with Mayer's hematoxylin.

**Flow Cytometric Analysis**

After transplantation, the recipient mouse spleens and allografted hearts were harvested under sterile conditions and gently sheared in a sterile cell dish. A single-cell suspension was obtained by passing the suspension through a 70-mesh cell sieve, and the erythrocytes were lysed using a red blood cell lysis buffer as described above. The cells were centrifuged at 1500 rpm for 5 min. at 4 °C and re-suspended in RPMI-1640 medium supplemented with 10% heat-inactivated fetal calf serum, 100 U/mL penicillin and 100 μg/mL streptomycin. These mononuclear cell suspensions were labeled with FITC-CD3, PE-conjugated CD4, APC-conjugated CD8 and BV510-conjugated CD25 monoclonal antibodies and subsequently subjected to FACS (Beckman Coulter, Brea, CA, USA) using the Cell Quest software (BD Biosciences, Mountain View, CA, USA).

**RNA-Sequencing**

PBMC cells were infected with shNC and shNF90. Total RNA was extracted with Trizol reagent. Sequencing was performed using Illumina HiSeqTM 2500 by Gene

Denovo Biotechnology Co. (Guangzhou, China).

### Statistical Analysis

Data were expressed as means ± standard deviation (SD) of at least three independent experiments. The results were analyzed by one-way analysis of variance (ANOVA) followed by Turkey test and student t-test. All statistical procedures were performed with GraphPad Prism Ver 5.0 software (GraphPad Software).

## Results

### NF45 and NF90 are nucleolar proteins that positively regulate rDNA transcription

Mass spectrometry has been used as a diagnostic tool to confirm the presence of both NF45 and NF90 in the nucleolar proteome (Wandrey et al, 2015). In the present study, the nucleolar enrichment of endogenous NF45 and NF90 proteins was confirmed by subcellular fractionation, an aggregate morphologywas observed to colocalize in the nucleolar markers fibrillarin and nucleolin, indicating that NF45 and NF90 are indeed nucleolar proteins (Figure 1A and Figure S1A). The primary function of a nucleolus is ribosome biogenesis (including the transcription of rRNAs from rDNAs), the folding, processing and modification of rRNAs, as well as the assembly of major ribosomal proteins. Intriguingly, the NF45/NF90 heterodimer was recently revealed as a novel regulator of ribosome biogenesis. A luciferase reporter containing the rDNA promoter was therefore used to assess the relationship between NF45/NF90 and rRNA synthesis. Inhibition of NF45/NF90 by siRNA downregulated the luciferase signal, whereas ectopic expression of NF45/NF90 enhanced luciferase activity, suggesting that NF45/NF90 is a positive regulator of rDNA synthesis (Figure 1B and Figure 1C).

Transcription of the 47S rRNA precursor, 47S pre-rRNA (comprised of the externally transcribed spacers 5′-ETS and 3′-ETS), is a rate-limiting step in ribosome biogenesis, which is followed by the cleavage of 47S pre-rRNA into several smaller rRNAs (18S, 5.8S and 28S rRNAs) (Tiku & Antebi, 2018). We therefore designed primers to target

the relevant regions of 47S pre-rRNA in order to measure its rate of transcription (Figure 1D). Consistent with the data from the rDNA promoter driven luciferase assay, real time-PCR analysis showed that silencing NF45 and NF90 significantly slowed down pre-rRNA transcription, and upregulation of NF45/NF90 dramatically strengthened the process (Figure 1E and Figure 1F). Silencing NF45/NF90 also suppressed nucleolar FUrd (fluorine-conjugated UTP analogue) incorporation (Figure S1B), further supporting the regulatory role of NF45/NF90 in rRNA synthesis.

It is known that within the NF45/NF90 heterodimer complex, NF90 contains a DZF motif (NF45 binding domain) and an NLS motif, as well as two RBD domains (RNA binding domains) which can directly bind RNA or DNA (Figure S2A). In order to investigate the involvement of the individual domains in rRNA synthesis, we inactivated the DZF and RBD domains using various point mutations (Figure S2A), and truncated the NLS motif to prevent its location in the nucleolus (Figs. S2B-2D). Interestingly, the DZF mutant completely reversed the effect of NF90 on transcription of pre-rRNA, indicating that binding to NF45 supports the NF90 regulation of rRNA synthesis (Figure S2E). Importantly, the NLS mutant also lost the ability to upregulate 47S pre-rRNA levels, demonstrating that the nucleolar localization of NF90 is required for moderating rRNA synthesis (Figure S2E). Surprisingly, the RBD mutant also resulted in the obvious translocation of NF90 from the nucleolus to the nucleoplasm, and downregulated 47S pre-rRNA levels by 12- and 7.7-fold compared to NF90 and the empty vector respectively (Figure S2E), suggesting that the RBD mutant of NF90 not only has a lower binding ability to rDNA and rRNA, but also serves as a dominant negative mutant to interfere with wild-type NF45/NF90 functions in the nucleolus.

**NF45/NF90 directly binds rDNA promoters by recognizing ARRE2 consensus sequences and regulates RNA Pol I transcription machinery**

To examine the protein occupancies of NF45 and NF90 at the rDNA loci, chromatin immunoprecipitation (ChIP) experiments were performed (Figure 2A). NF45 and NF90 binding were enhanced by approximately 3–5.2-fold, and 3.8–8.7-fold respectively,

compared with the IgG control (Figure 2B), suggesting that NF45/NF90 might regulate rDNA transcription through direct binding to the rDNA loci, especially the rDNA promoter region (H42.9). Since the NF45/NF90 complex has been shown to recognize upstream ARRE2 in the human IL-2 promoter (Shi et al, 2007b), we analyzed the rDNA promoter region using MatInspector (Genomatix), and found it also harbored two putative ARRE2-like sequences (*GGAAA*) at nucleotide positions −795 to −799, and −1760 to −1756 from the transcription start site (Figure 2C). As expected, an electrophoretic mobility shift assay (EMSA) and luciferase assay confirmed that the AARE2 elements at the rDNA promoter loci are required for NF90 interaction and regulation of rDNA promoter activity (Figure 2D and Figure 2E).

The regulatory mechanism of rDNA transcription requires the synergistic transaction of UBF followed by promoter selectivity factor 1 (SL1) in order to recruit RNA polymerase I (Pol I) to sit on the rDNA promoter (Figure 3A) (Friedrich et al, 2005). Interestingly, in a co-immunoprecipitation (co-IP) assay, NF45/NF90 had a stronger binding affinity with UBF1 than a panel of other major nucleolar proteins including S5, L9, B23 and C23 (Figure 3B and Figure 3C). As UBF1 activity correlates with phosphorylation and ubiquitination (Zhang et al, 2011), the NF45 and NF90 proteins in HEK293 cells were silenced in order to test their involvement in UBF1 post-translational modification. In separate experiments, both NF45 and NF90 knockdown decreased the expression level of total UBF1 and its phosphorylation (Ser388) upon serum stimulation (Figure 3D), but upregulated the ubiquitination level of UBF1 (Figure S3A and Figure S3B). This indicated that depleting NF45/NF90 suppresses UBF1 transcriptional activity by inhibiting its phosphorylation and promoting its ubiquitin-dependent degradation. Since UBF activates Pol I to promote rDNA transcription, RNA pol I levels were also examined upon depletion of NF45/NF90. A relative downregulation of RNA pol I expression in siNF45/NF90 cells was observed (Figure 3D), further suggesting that the NF45/NF90 complex positively regulates UBF1 to recruit RNA pol I to sit on the rDNA promoter.

Previous studies have shown that rDNA transcription can be activated in serum-deprived cells when re-subjected to serum stimulation. To investigate the effects of rRNA transcription on NF45/NF90 localization and function, a ChIP assay was performed. The binding ability of NF45/NF90 to the rDNA promoter was significantly increased following serum stimulation (Figure 3E). CX5461 (Drygin et al, 2011), a highly specific Pol I inhibitor that can suppress rDNA transcription by preventing Pol I-specific transcription initiation factors binding to the rDNA promoter to determine the relationship of NF45/NF90 localization and rDNA transcription, was also investigated. In agreement with our hypothesis, the binding ability of NF45/NF90 to the rDNA loci was markedly decreased following treatment with CX5461 (Figure 3F). Interestingly, immunofluorescence analysis revealed a strong translocation of NF45 and NF90 from the nucleolus to the nucleoplasm following CX5461 treatment (Figure 3G), suggesting that the subcellular location of NF45/NF90 is associated with the Pol I driven transcription machinery.

## NF45/NF90-mediated rDNA transcription contributes to calcineurin-NFAT-mediated T cell activation *in vitro*

NF45/NF90 was originally isolated in activated Jurkat T cells and is believed to be involved in T cell activation, but the specific mechanism has yet to be fully elucidated (Kao et al, 1994). Here, we postulate that NF45/NF90-mediated rDNA transcription contributes to T cell activation and proliferation. In agreement with our hypothesis, there was a strong increase of NF45 and NF90 binding to the rDNA promoter when $CD3^+$ T cells were activated with the calcineurin-NFAT stimulators PMA and ionomycin (P/I) (Figure 4A). We also noticed that P/I significantly induced 47S pre-rRNA transcription (Figure 4B), and that this was substantially suppressed by NF45/NF90 knockdown (Figure 4C). In agreement with the change in 47S pre-rRNA levels, RNA-seq revealed that among 161 differentially expressed genes related to ribosome biogenesis ($\geq$ 2-fold difference), 80% of genes were upregulated upon P/I treatment in $CD3^+$T cells, thereby confirming that P/I treatment activates general

ribosome biogenesis pathways (Figure S4A). As expected, NF90 knockdown undoubtedly suppressed the P/I-stimulated increase in a panel of genes related to ribosome biogenesis (78% among 64 ribosome biogenesis-related differentially expressed genes) (Figure S4B).

When T cell activation was blocked by FK506, NF45 and NF90 translocated from the nucleolus to the nucleocytoplasm and cytoplasm, respectively (Figure S5A). This was accompanied by dramatic reductions of NF45/NF90 binding to the rDNA gene loci and 47S pre-rRNA expression (Figure S5B and Figure S5C). To elucidate how the calcineurin-NFAT pathway is involved in NF45/NF90-mediated rDNA transcription, NFAT expression upon T cell activation was examined. Surprisingly, immunofluorescence analysis revealed that NFATc2 translocated from the cytoplasm into the nucleoplasm, and also enriched in the nucleolus upon P/I induced T cell activation (Figure 4D). Furthermore, confocal microscopy and co-IP results showed that both NF45 and NF90 co-localized and interacted with NFATc2 in activated T cells (Figs. 4D-4F), suggesting that NFAT might interact with the NF45/NF90 complex to coordinatively regulate rDNA transcription in the nucleoli for T cell activation.

Next, we questioned whether silencing NF45 or NF90 in T cells would lead to an inhibition of T cell activation. Fluorescence-activated cell sorting analysis (FACS) results suggested that, in the presence of P/I stimulation, NF45/NF90 knockdown significantly inhibited the expression of CD69, an early marker of T cell activation (Figure 5A, and Figure S6A). Consistent with this, the mRNA and protein expression of IL-2 and NF-kB together with IFN-γ secretion were also reduced in shNF45 and shNF90 T cells (Figure 5B and Figure S6B-6C). Peripheral blood mononuclear cells (PBMC) with NF45 or NF90 inhibition were also found to have a lower proliferation rate following P/I stimulation (Figure 5C). Considered together, these data suggest NF45/NF90-rDNA transcription is involved in T cell activation and proliferation.

Based on the above observations it is conceivable that T cell proliferation and activation

require cooperation between NFAT-mediated cell factors (such as IL-2 and IFN-γ) and NF45/NF90-mediated ribosomal biogenesis. Thus, inhibiting ribosomal biogenesis might be an alternative pathway to suppress T cell proliferation and activation. CX5461 is a specific rRNA synthesis inhibitor that selectively inhibits Pol I-driven rRNA transcription and ribosomal biogenesis, but has no effect on Pol II (Drygin et al, 2011). Thus, the effects of CX5461 on T cell activation and proliferation were investigated. Similar to FK506, CX5461 also significantly suppressed the P/I-induced nuclear translocation of NFATc2 from the cytoplasm (Figure 5D). Next, T cells were treated with P/I in combination with either FK506 or CX5461 for 6 h. It was found that both CX5461 and FK506 reduced the expression of CD69, IL-2 and NF-kB, as well as the proliferation of T cells (Figs. 5E-5G and Figs. S7A-7C). Intriguingly, CX5461 had a more dramatic inhibitory effect on T cell activation and proliferation when compared to FK506, further supporting the key contribution of NFAT-NF45/NF90-mediated ribosomal biogenesis in T cell activation.

## CX5461 is an effective immunosuppressant and prolongs allograft survival

T cell activation is one of the key events in acute allograft rejection. It was found that the pre-rRNA level of T cells from recipient mouse spleens were significantly higher in the acute rejection group than in the negative control (NC) group for both skin and heart transplant mouse models (Figure 6A). In order to prosecute this observation in a clinical context, PBMC from renal transplant patients was collected and its pre-rRNA levels were measured. The pre-rRNA levels in T cell-mediated rejection (TCMR) patients were significantly higher than both in antibody-mediated rejection (ABMR) patients and in non-rejection patients after transplantation (Figure 6B). All of these results support the conclusion that pre-rRNA transcriptional activation plays a key role in T cell activation during allograft rejection.

In order to investigate the feasibility of ribosome biogenesis as a target for the

development of immune agents, allogeneic skin graft mice were treated with 2.0 mg•kg$^{-1}$ FK506, the most commonly used immunosuppressive drug, and different doses of CX5461 (0.5, 1.0, and 2.0 mg•kg$^{-1}$, respectively) over a therapeutic window of 30 days (Figure 6C). The body weight of CX5461-treated mice did not change significantly compared to dimethyl sulfoxide- (DMSO) treated control mice, indicating no obvious systemic toxicity for the applied doses (Figure S8A). However, the FK506 group exhibited obvious weight loss, and both sparse and shedding hair around the eyes during treatment, indicating strong off-target activity (i.e. toxicity) in the recipient mice. Obvious skin graft rejection was observed in DMSO-control mice from five days after skin transplantation, whereas CX5461 treated mice showed significantly prolonged recipient skin survival in a dose-dependent manner (Figure 6D). Interestingly, treatment with 1.0 mg•kg$^{-1}$ CX5461 resulted in similar therapeutic kinetics compared to treatment with 2.0 mg•kg$^{-1}$ FK506, and treatment with 2.0 mg•kg$^{-1}$CX5461 had a stronger effect than treatment with FK506 at the same concentration (Figure 6D). Histological examination of graft skins showed massive inflammatory infiltration, obvious edema, and tissue necrosis in the control group. These phenomena were significantly relieved following CX5461 treatment in a dose-dependent manner, which was also observed in FK506-treated mice (Figure 6E). At the end of the experiment, the mice were sacrificed, and the skin grafts, spleens, and thymuses were separated for further analysis. Significant weight loss was observed only in the thymuses, but not the spleens, in the FK506- and CX5461-treated groups (Figure S8B), indicating both CX5461 and FK506 cause thymus-specific suppressing activity. Next, mononuclear cells from the spleens were isolated, and then labeled them with FITC-CD3, PE-conjugated CD4, and APC-conjugated CD8 monoclonal antibodies for FACS analysis. Treatment with CX5461 decreased the relative percentage of both $CD4^+$ and $CD8^+$ T cells in a dose-dependent manner. In both cases, 1.0 and 2.0 mg•kg$^{-1}$ doses of CX5461 were more effective than treatment with FK506 at the same concentrations (Figure 6F). Commensurate with both these observations and the *in vitro* results, a dose-dependent decrease of both IFN-γ and IL-12 levels in the serum of recipient mice was observed upon treatment with 1.0 and 2.0 mg•kg$^{-1}$ CX5461. Treatment with FK506 at the same concentrations was less

effective (Figure 6G and 6H).

Recent advances have made the heart transplantation model an excellent tool for quantifying immune rejection by monitoring palpations of the grafted heart (Costello et al, 2018). Heart graft mice were further treated with 2.0 mg•kg$^{-1}$ FK506 and 2.0 mg•kg$^{-1}$ CX5461, which was the most effective concentration in the skin graft experiments. It was found that CX5461-treated allografts survived significantly longer (>80 days, animals with live transplants at day 80 were executed, the prescheduled experimental endpoint) than DMSO-treated allografts (6.6±0.5 days) and FK506-treated allografts (41.4±13.7 days) (Figure 6I). Similar to skin transplantation experiments, CX5461 treatment had no influence on mouse body weight or other obvious toxic outcomes (Figure S9A). Similar to skin-graft mice, the FK506 group also exhibited weight loss, coarse and pale hairs, and molting around the eyes during treatment, indicating side effects or drug toxicity in the recipient mice (Figs. S9A and S9B). The hearts, neck lymph nodes and spleens in the DMSO group were significantly larger and heavier than the FK506 and CX5461 groups (Figs. S9C and S9D). The DMSO-treated group showed severe inflammatory cell infiltration and myocardial necrosis in a histological analysis, whereas the FK506 and CX5461-treated groups showed less lymphocyte infiltration and almost normal tissue structure (Figure 6J). Immunohistochemistry analysis further revealed that CX5461 treatment drastically reduced the infiltration of CD3$^+$ T cells (Figure 6J). Furthermore, treatment with CX5461 decreased the relative percentages of CD4$^+$ and CD8$^+$ T cells in the lymphocytes of heart grafts, an effect which was more pronounced than treatment with FK506 at the same concentration (Figure 6K). As expected, CX5461 and FK506 treatment reduced the expression of granzyme B, IL-12, and TNF-α mRNA (Figs. 6L-N,), adding further impetus to the use of CX5461 as an effective immunosuppressive agent.

As regulatory T cells (Tregs) play an important role in alloimmune tolerance (Alijotas-Reig et al, 2014), the CD4$^+$CD25$^+$ Treg cell populations isolated from cervical lymph

nodes were examined. As expected, CX5461 was a stronger enhancer of $CD4^+CD25^+$ Treg cell populations than FK506 (Figure 6O), indicating that CX5461 contributes to immune suppression in the allograft microenvironment partially through regulatory T cell mechanisms. Importantly, pre-rRNA was highly expressed in the spleen lymphocytes of transplanted groups (DMSO) compared to NC mice, whereas near complete inhibition was observed when these transplanted mice were treated with CX5461 and FK506 (Figure 6P). These results suggest that CX5461 suppression of T cell activation during allograft rejection is associated with its inhibitory effect on rDNA transcription.

## Discussion

In recent years, the NF45/NF90 protein heterodimer has been implicated in a wide variety of biological processes in mammals (Wu et al, 2019). NF45/NF90 was previously identified by mass spectrometry to recognize the upstream ARRE2 consensus sequence of the IL-2 promoter in activated T cells, and thus NF45/NF90 is speculated to mediate T cell activation by regulating IL-2 transcription (Shi et al, 2007a). Herein, we postulate that the main contribution of NF45/NF90 to T cell activation occurs through the regulation of rDNA transcription, as opposed to IL-2 transcription, for the following reasons. 1) NF45/NF90 is predominantly enriched in the nucleolus, where there are two ARRE2 consensus sequences in the rDNA promoter region. 2) ChIP, EMSA and luciferase assays confirmed that NF45/NF90 associates with both AARE2 elements of the rDNA promoter (Figs. 2B-E). 3) ChIP data (Figure 2B and Figure S10) show that the binding affinity of NF45/NF90 to the rDNA promoter is 4–8 fold higher than the IgG control; substantially higher than the 1.5–2 fold upregulation in the binding affinity of NF45/NF90 with the IL-2 promoter when compared to the IgG control. 5) Finally, P/I stimulation did not significantly alter the binding affinity of NF45/NF90 to the IL-2 promoter (Figure S10), but significantly enhanced the association of NF45/NF90 with the rDNA promoter and increased subsequent downstream T cell activation (Figure 4A and Figure 5B).

Ribosome biogenesis is a complex process that requires coordinated transcription and processing of 47S pre-rRNA, the translation, folding, modification, and binding of ribosomal proteins, as well as the assembly and the nucleolar export of the 40S and 60S subunits into the cytoplasm (Strunk et al, 2011). A previous study showed that the NF45/NF90 heterodimer binds to the pre-60S ribosome subunit and supports subunit assembly and maturation in the late stages of ribosome biogenesis (Wandrey et al, 2015). It is known that the transcription of 47S pre-rRNA is a rate-limiting step in ribosome biogenesis. The assembly of a specific multiprotein complex containing at least UBF, SL1, and transcription initiation factor I (TIF-I) at the rDNA promoter is necessary for the initiation of 47S pre-rRNA synthesis in mammals (Derenzini et al, 2017) (Figure 3A). In this study, we found that NF45/NF90 directly binds the rDNA promoter and mediates the interaction of UBF with the rDNA promoter, thus promoting the recruitment of RNA Pol I to the rDNA promoter regions (Figure 5H). Overexpressing NF45/NF90 enhanced rDNA promoter activity and 47S pre-rRNA expression, whereas inhibiting NF45/NF90 significantly suppressed these processes (Figs. 1B-1F). Both nucleolar localization (Figure 1A) and rDNA binding (Figure 2B) of NF90 are required for its role in the transcription of pre-rRNA. Notably, overexpressing NF90 is insufficient to promote pre-rRNA synthesis without binding NF45, suggesting that there is a synergy between NF45 and NF90 in pre-rDNA transcription.

Importantly, we found that NF45/NF90-mediated rDNA transcription contributes to T cell activation. P/I stimulation triggered the translocation of NFAT to from the cytoplasm to the nucleolus causing it to interact with NF45/NF90 (Figure 4D), thereby promoting its binding to the rDNA promoter (Figure 4A) and rDNA transcription level (Figure 4C). This suggested that NFAT and NF45/NF90 might collaborate to promote rDNA transcription and ribosomal biogenesis upon T cell activation. In agreement with this hypothesis, the calcineurin inhibitor FK506 significantly inhibited the nucleolar location of NF45/NF90, its rDNA binding ability and its capacity to drive rDNA transcription (Figure S5). More importantly, NF45/NF90 knockdown significantly

suppressed P/I-induced rDNA transcription, and T cell activation and proliferation (Figure 5), indicating that P/I-induced rDNA transcription is dependent on NF45/NF90 and is necessary for T cell activation. Herein, we demonstrated that NF45/NF90-mediated rDNA transcription and ribosomal biogenesis is a novel signaling pathway essential for T cell activation, which synergistically activates T cells *via* the classic calcineurin-NFAT-cytokine pathway. Moreover, we found that NF45/NF90 is a key signaling molecule that mediates the classical calcineurin-NFAT signaling pathway and ribosomal biogenesis (Figure 5H).

CsA and FK506 are two of the most commonly used immunosuppressants in the clinic, but they suffer from side effects, which may be due to intrinsic toxicity or more likely the result of the general inhibition of calcineurin, which plays other biologically important roles besides NFAT activation (Lee et al, 2020). It is therefore necessary to develop new immunosuppressive agents based on new targets. Even though ribosome biogenesis occurs in all cells, there is evidence that the selective inhibition of ribosome biogenesis may, in some instances, result in a selective controlling the cell cycle progression to proliferating cells (Derenzini et al, 2017). In the process of organ transplantation or autoimmune diseases, T cells are overactivated, which requires the close cooperation of ribosome biogenesis. As expected, we found that the pre-rRNA levels of T cells in both mouse skin and heart allograft rejection models were significantly higher than in the NC group (Figure 6A). Intriguingly, we also found that the pre-rRNA levels in TCMR patients were also significantly higher than in both ABMR patients and in non-rejection patients after renal transplantation (Figure 6B). Thus, targeting ribosome biogenesis may be a general mechanism to inhibit T cell overactivation and provide an additional therapeutic strategy for immunosuppression.

Excitingly, we found CX5461, a specific rDNA transcription inhibitor, showed much stronger inhibitory effects than FK506 on T cell activation and proliferation *in vitro* and *in vivo*, and was a more potent preventor of allograft rejection in skin and heart allograft models with lower side effects. For example, CX5461-treated heart allografts survived

significantly longer (>80 days) than DMSO-treated allografts (6.6±0.5 days) and FK506-treated allografts (41.4±13.7 days). In addition, CX5461 treatment also suppressed P/I-triggered NFAT entry into the nucleus, indicating that rDNA transcription inhibition might have a feedback effect on NFAT activation (Figure 5D and Figure 5H). This suggests that CX5461 may be a promising immunosuppressant for organ transplant rejection or autoimmune diseases.

In summary, we revealed NF45/NF90-mediated rDNA transcription as a novel signaling pathway essential for T cell activation, and as a new target for the development of safe and effective immunosuppressants.

## Acknowledgements

**Funding:**

- This research was supported by the National Natural Science Foundation of China (81702750, 81670141 and 81970145);
- Natural Science Foundation of Guangdong Province (2020A1515011465);
- Science, Technology & Innovation Commission of Shenzhen Municipality (JCYJ20170818164756460, JCYJ20180307154700308, JCYJ20170818163844015, JCYJ20180307151420045 and JCYJ20190807151609464);
- China Postdoctoral Science Foundation (2018M643299);
- The Social Development Foundation of Jiangsu Province (BE2018691);
- Sigrid Jusélius foundation in Finalnd.

## References

Alijotas-Reig J, Llurba E, Gris JM (2014) Potentiating maternal immune tolerance in pregnancy: a new challenging role for regulatory T cells. *Placenta* **35:** 241-248

Barber GN (2009) The NFAR's (nuclear factors associated with dsRNA) Evolutionarily

conserved members of the dsRNA binding protein family. *Rna Biol* **6:** 35-39

Borroto A, Reyes-Garau D, Jimenez MA, Carrasco E, Moreno B, Martinez-Pasamar S, Cortes JR, Perona A, Abia D, Blanco S, Fuentes M, Arellano I, Lobo J, Heidarieh H, Rueda J, Esteve P, Cibrian D, Martinez-Riano A, Mendoza P, Prieto C, Calleja E, Oeste CL, Orfao A, Fresno M, Sanchez-Madrid F, Alcami A, Bovolenta P, Martin P, Villoslada P, Morreale A, Messeguer A, Alarcon B (2016) First-in-class inhibitor of the T cell receptor for the treatment of autoimmune diseases. *Science translational medicine* **8:** 370ra184

Broere F, van Eden W (2019) T cell subsets and T cell-mediated immunity. In *Nijkamp and Parnham's Principles of Immunopharmacology*, pp 23-35. Springer

Castella S, Bernard R, Corno M, Fradin A, Larcher JC (2015) Ilf3 and NF90 functions in RNA biology. *Wiley Interdisciplinary Reviews: RNA* **6:** 243-256

Chikamatsu K, Sakakura K, Whiteside TL, Furuya N (2007) Relationships between regulatory T cells and CD8+effector populations in patients with squamous cell carcinoma of the head and neck. *Head Neck-J Sci Spec* **29:** 120-127

Costello R, Kissenpfennig A, Martins PN, McDaid JJEoodd (2018) Development of transplant immunosuppressive agents–considerations in the use of animal models. **13:** 1041-1053

Derenzini M, Montanaro L, Trere D (2017) Ribosome biogenesis and cancer. *Acta histochemica* **119:** 190-197

Drygin D, Lin A, Bliesath J, Ho CB, O'Brien SE, Proffitt C, Omori M, Haddach M, Schwaebe MK, Siddiqui-Jain A (2011) Targeting RNA polymerase I with an oral small molecule CX-5461 inhibits ribosomal RNA synthesis and solid tumor growth. *Cancer*

*Res* **71:** 1418-1430

Friedrich JK, Panov KI, Cabart P, Russell J, Zomerdijk JC (2005) TBP-TAF complex SL1 directs RNA polymerase I pre-initiation complex formation and stabilizes upstream binding factor at the rDNA promoter. *J Biol Chem* **280:** 29551-29558

Grandori C, Gomez-Roman N, Felton-Edkins ZA, Ngouenet C, Galloway DA, Eisenman RN, White RJ (2005) c-Myc binds to human ribosomal DNA and stimulates transcription of rRNA genes by RNA polymerase I. *Nat Cell Biol* **7:** 311-318

Group CSC, Haynes R, Blackwell L, Staplin N, Herrington WG, Emberson J, Judge PK, Storey BC, Landray MJ, Harden PN (2018) Campath, calcineurin inhibitor reduction, and chronic allograft nephropathy (the 3C Study)–results of a randomized controlled clinical trial. *American Journal of Transplantation* **18:** 1424-1434

Guan D, Altan-Bonnet N, Parrott AM, Arrigo CJ, Li Q, Khaleduzzaman M, Li H, Lee C-G, Pe'ery T, Mathews MB (2008) Nuclear factor 45 (NF45) is a regulatory subunit of complexes with NF90/110 involved in mitotic control. *Mol Cell Biol* **28:** 4629-4641

Hacot S, Coute Y, Belin S, Albaret MA, Mertani HC, Sanchez JC, Rosa-Calatrava M, Diaz JJ (2010) Isolation of nucleoli. *Current protocols in cell biology* **47:** 3.36. 31-33.36. 10

Idda ML, Lodde V, Galleri G, Martindale JL, Munk R, Abdelmohsen K, Cucca F, Gorospe M (2019) NF90 regulation of immune factor expression in response to malaria antigens. *Cell Cycle* **18:** 708-722

Jain J, McCaffrey PG, Miner Z, Kerppola TK, Lambert JN, Verdine GL, Curran T, Rao A (1993) The T-cell transcription factor NFATp is a substrate for calcineurin and interacts with Fos and Jun. *Nature* **365:** 352-355

Kao PN, Chen L, Brock G, Ng J, Kenny J, Smith AJ, Corthesy B (1994) Cloning and expression of cyclosporin A- and FK506-sensitive nuclear factor of activated T-cells: NF45 and NF90. *J Biol Chem* **269:** 20691-20699

Kiesler P, Haynes PA, Shi L, Kao PN, Wysocki VH, Vercelli D (2010) NF45 and NF90 regulate HS4-dependent interleukin-13 transcription in T cells. *J Biol Chem* **285:** 8256-8267

Lahiri DK, Ge Y-W (2000) Electrophoretic mobility shift assay for the detection of specific DNA–protein complex in nuclear extracts from the cultured cells and frozen autopsy human brain tissue. *Brain Research Protocols* **5:** 257-265

Lee H-G, Kim L-K, Choi J-M (2020) NFAT-Specific Inhibition by dNP2-VIVIT Ameliorates Autoimmune Encephalomyelitis by Regulation of Th1 and Th17. *Molecular Therapy-Methods & Clinical Development* **16:** 32-41

Masuda K, Kuwano Y, Nishida K, Rokutan K, Imoto I (2013) NF90 in Posttranscriptional Gene Regulation and MicroRNA Biogenesis. *Int J Mol Sci* **14:** 17111-17121

Monostory K (2018) Metabolic Drug Interactions with Immunosuppressants. *Organ Donation and Transplantation: Current Status and Future Challenges***:** 409

Nelson JD, Denisenko O, Bomsztyk K (2006) Protocol for the fast chromatin immunoprecipitation (ChIP) method. *Nature protocols* **1:** 179-185

Okeefe SJ, Tamura J, Kincaid RL, Tocci MJ, Oneill EA (1992) Fk-506-Sensitive and Csa-Sensitive Activation of the Interleukin-2 Promoter by Calcineurin. *Nature* **357:** 692-694

Parker LM, Fierro-Monti I, Mathews MB (2001) Nuclear factor 90 is a substrate and regulator of the eukaryotic initiation factor 2 kinase double-stranded RNA-activated protein kinase. *J Biol Chem* **276:** 32522-32530

Peng Q, Wu J, Zhang Y, Liu Y, Kong R, Hu L, Du X, Ke Y (2010) 1A6/DRIM, a novel t-UTP, activates RNA polymerase I transcription and promotes cell proliferation. *Plos One* **5:** e14244

Shamanna RA, Hoque M, Lewis-Antes A, Azzam EI, Lagunoff D, Pe'ery T, Mathews MB (2011) The NF90/NF45 Complex Participates in DNA Break Repair via Nonhomologous End Joining. *Mol Cell Biol* **31:** 4832-4843

Shi L, Godfrey WR, Lin J, Zhao G, Kao PN (2007a) NF90 regulates inducible IL-2 gene expression in T cells. *The Journal of experimental medicine* **204:** 971-977

Shi L, Qiu D, Zhao G, Corthesy B, Lees-Miller S, Reeves WH, Kao PN (2007b) Dynamic binding of Ku80, Ku70 and NF90 to the IL-2 promoter in vivo in activated T-cells. *Nucleic Acids Res* **35:** 2302-2310

Shim J, Lim H, Yates III JR, Karin M (2002) Nuclear export of NF90 is required for interleukin-2 mRNA stabilization. *Mol Cell* **10:** 1331-1344

Skeens MA, Dietrich MS, Ryan-Wenger N, Gilmer MJ, Mulvaney SA, Akard TF (2019) The Medication Level Variability Index (MLVI) as a potential predictive biomarker of graft-versus-host disease in pediatric hematopoietic stem cell transplant patients. *Pediatric transplantation* **23:** e13451

Strunk BS, Loucks CR, Su M, Vashisth H, Cheng S, Schilling J, Brooks CL, 3rd, Karbstein K, Skiniotis G (2011) Ribosome assembly factors prevent premature

translation initiation by 40S assembly intermediates. *Science* **333:** 1449-1453

Tiku V, Antebi A (2018) Nucleolar function in lifespan regulation. *Trends in cell biology* **28:** 662-672

Wandrey F, Montellese C, Koos K, Badertscher L, Bammert L, Cook AG, Zemp I, Horvath P, Kutay U (2015) The NF45/NF90 Heterodimer Contributes to the Biogenesis of 60S Ribosomal Subunits and Influences Nucleolar Morphology. *Mol Cell Biol* **35:** 3491-3503

Wolkowicz UM, Cook AG (2012) NF45 dimerizes with NF90, Zfr and SPNR via a conserved domain that has a nucleotidyltransferase fold. *Nucleic Acids Res* **40:** 9356-9368

Wu T-H, Shi L, Lowe AW, Nicolls MR, Kao PN (2019) Inducible expression of immediate early genes is regulated through dynamic chromatin association by NF45/ILF2 and NF90/NF110/ILF3. *Plos One* **14**

Zhang Y, Forys JT, Miceli AP, Gwinn AS, Weber JD (2011) Identification of DHX33 as a mediator of rRNA synthesis and cell growth. *Mol Cell Biol* **31:** 4676-4691

Zhao GH, Shi LF, Qiu DM, Hu H, Kao PN (2005) NF45/ILF2 tissue expression, promoter analysis, and interleukin-2 transactivating function. *Exp Cell Res* **305:** 312-323

# Figures legend

**Figure1 NF45/NF90 is a nucleolar protein complex that positively regulates rDNA transcription.** (A) Confocal images of HeLa cells stained with NF45/NF90 antibodies and antibodies against nucleolin and fibrillarin. Scale bar, 10 μm. (B) Control siRNA (NC), siRNAs of NF45/NF90 (siNF45#1, siNF45#2, siNF90#1 and siNF90#2) were transfected into HEK293 cells for 24 h, and then PHrD-IRES-Luc was co-transfected into the cells. Luciferase activity was measured after a further 24 h. (C) Empty vector (EV), NF45-flag plasmid (NF45) or NF90-flag plasmid (NF90) were transfected into HEK293 cells for 24 h, and then PHrD-IRES-Luc was co-transfected into the cells. Luciferase activity was measured after a further 24 h. (D) Arrows indicate qPCR primer positions on the 47S pre-rRNA. (E and F) qPCR analysis of 47S pre-rRNA from HEK293 cells transfected with indicated siRNAs (E) and plasmids (F) for 24 h. Bar = mean ± SD， n=3. (*P<0.05, ***P<.001)

**Figure 2. NF45/NF90 preferentially binds to the promoter region of the rDNA gene loci by directly recognizing ARRE consensus sequences.** (A) Schematic illustration of a single human rDNA repeat and positions of the primers used for ChIP. (B) In Jurkat cells, a ChIP assay was performed with control IgG, NF45 NF90 antibodies, and then the precipitated DNA was analyzed using qPCR with the aforementioned primers. The relative rDNA fold-enrichment was normalized to control IgG treatment. (C) The human rDNA promoter region contains two putative NF90-binding sites (colored red). The grey box indicates the rDNA promoter probe in panel D. (D) EMSA data from nuclear extracts of HEK293 cells using the details described in Materials and Methods section. (E) The relative luciferase activity of HEK293T cells transfected with empty vector (EV) or Flag-NF90 (NF90) in combination with wild type (WT) or ARRE-mutated rDNA-Luc reporter plasmids (Mutant) for 24 h.

**Figure 3. NF45/NF90 affects rDNA transcription as a positive regulatory factor by recruiting and regulating UBF1 activity.** (A) The regulatory mechanism of the rDNA transcription. Firstly, the core promoter trans-acting element UBF1 binds to the rDNA promoter

to recruit SL1, then SL1 recruits Pol I for rDNA transcription. (B) Co-IP analysis of nucleolar proteins with NF45 and NF90 in HEK293 cells were transfected with EV, and the following plasmids: GFP-S5, GFP-L9, GFP-B23, GFP-UBF, GFP-C23. * for the target protein. (C) Co-IP analysis of UBF with NF45 and NF90 in HEK293 cells. (D) HEK293 cells were transfected with NF45-specfic siRNAs, NF90-specfic siRNAs, and then cells were stimulated in serum for 0, 3 and 6 h. Cell lysates were prepared at 48 h post-transfection to analyze NF45/NF90 levels by western blotting. (E) ChIP analysis was used to determinate the binding ability of NF45 and NF90 to rDNA promoters in Jurkat cells stimulated with serum for 0, 3 and 6 h. (F) ChIP analysis of NF45 and NF90 binding to the H42.9 loci in Jurkat cells with the treatment of CX5461 or DMSO for 2 h. (G) Confocal images of Jurkat cells treated with CX5461 for 2 h showing NF45 and NF90 colocalized with fibrillarin in nucleoli. Scale bar, 10 μm. In all panels, bar = mean ± SD，n=3.

**Figure 4. NF45/NF90-mediated rDNA transcription contributes to T cell activation by interacting with NFATc2 in the nucleolus.** (A) ChIP analysis of NF45 and NF90 binding to the H42.9 loci in $CD3^+$ T cells stimulated with P/I for 6 h. (B) qPCR analysis of pre-rRNA in $CD3^+$ T cells treated with P/I for 6 h. (C) $CD3^+$ T cells were first silenced with negative shRNA (shNC), NF45 shRNAs (sh45) or NF45 shRNAs (sh90), and then treated with P/I to extract total RNA for qPCR analysis of pre-rRNA. (D) Confocal images of Jurkat cells to show NF45 (left panel) or NF90 (right panel) (green fluorescence) colocalized with NFATc2 (red fluorescence) in nucleoli. Scale bar, 10 μm. (E) Co-IP analysis of NFATc2 with NF45 and NF90 in Jurkat cells. (F) ChIP analysis of NFATc2 binding to the rDNA loci in CD3+ T cells stimulated with P/I (PMA/Ionomycin) for 6 h.

**Figure 5. NF45/NF90-mediated rDNA transcription is necessary for cell proliferation and activation.** (A) CD69 expression, an early marker of lymphocyte activation, in $CD3^+$ T cells upon stimulation with P/I for 6 h. (B) qPCR analysis of IL-2 mRNA expression from samples in panel E. (C) The proliferation of PBMC was monitored using a CCK-8 assay. (D) Confocal images to show the subcellular localization of NFATc2 in $CD3^+$ T cells treated with P/I and FK506 or CX5461. Scale bar, 10 μm. (E) Flow cytometry

analysis of CD69 expression in P/I-stimulated $CD3^+$ T cells treated with or without FK506 or CX5461. (F) qPCR analysis of IL-2 mRNA expression in $CD3^+$ T cells with the indicated treatments. (G) Flow cytometry analysis of CFSE-labeled CD3+ T cells in the presence of DMSO, FK506 and CX5461 for 0, 3 and 7 d. (H) Schematic diagram: NF45/NF90-mediated rDNA transcription coordinates with NFAT signaling in regulating T cell activation. In all panels, bar = mean ± SD，n=3, $*P < 0.05$, $**P < 0.01$, $***P < 0.001$.

**Figure 6. CX5461 promotes graft survival in skin and cardiac allograft models.** (A) qPCR analysis of pre-rRNA expression from skin- and heart-transplanted mouse spleens. (B) pre-rRNA expression levels of PBMC from renal transplantation patients. (Stable group, n=7. ABMR group, n=8. TCMR group, n=8). (C) Therapeutic scheme showing the daily administration of CX5461 or FK506 in skin- and cardiac-allografted mice until day 80. (D) Skin graft survival curve in mice treated with DMSO, 2.0 mg/kg FK506 or 0.5–2.0 mg/kg CX5461. At least five mice from each group were used in the experiments. (E) Representative images of HE staining of skin graft at seven days post transplantation. Scale bar = 50 μm. (F) FACS analysis of spleen T cells labeled with CD3, CD4 and CD8 antibodies. (G and H) ELISA analysis of IL-12 and IFN-γ levels in recipient mouse serum at four days post transplantation. (I) The survival time (days) of cardiac graft in mice treated with DMSO, 2.0 mg/kg FK506 or 2.0 mg/kg CX5461. At least five mice from each group were used in the experiments. (J) Representative images of HE and CD3-IHC staining of cardiac graft at seven days post transplantation. Scale bar = 100 μm. (K) FACS analysis of isolated mononuclear cells from transplanted heart labeled with CD3, CD4 and CD8 antibodies. (L-N) qPCR analysis of mRNA expression levels of granzyme B, IL-12 and TNF-α from heart-transplanted mouse spleens. (O) FACS analysis of isolated mononuclear cells from heart-transplanted mouse lymph nodes labeled with CD25 and CD4 antibodies. (P) qPCR analysis of pre-rRNA expression from transplanted mouse spleen. Bar = 50 μm, mean ± SEM，n=5. In all panels, $***P < 0.001$.

# Figures

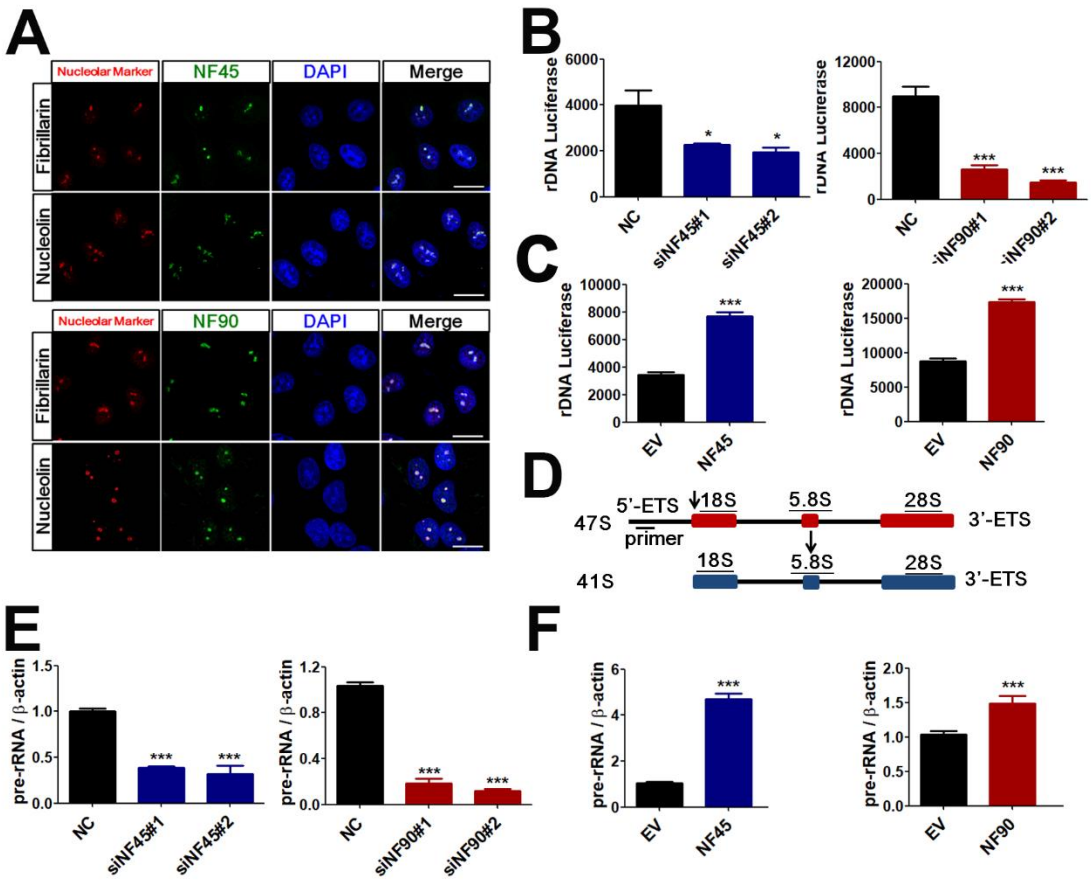


**Figure 1. NF45/NF90 is a nucleolar protein complex that positively regulates rDNA transcription.** (A) Confocal images of HeLa cells stained with NF45/NF90 antibodies and antibodies against nucleolin and fibrillarin. Scale bar, 10 μm. (B) Control siRNA (NC), siRNAs of NF45/NF90 (siNF45#1, siNF45#2, siNF90#1 and siNF90#2) were transfected into HEK293 cells for 24 h, and then PHrD-IRES-Luc was co-transfected into the cells. Luciferase activity was measured after a further 24 h. (C) Empty vector (EV), NF45-flag plasmid (NF45) or NF90-flag plasmid (NF90) were transfected into HEK293 cells for 24 h, and then PHrD-IRES-Luc was co-transfected into the cells. Luciferase activity was measured after a further 24 h. (D) Arrows indicate qPCR primer positions on the 47S pre-rRNA. (E and F) qPCR analysis of 47S pre-rRNA from HEK293 cells transfected with indicated siRNAs (E) and plasmids (F) for 24 h. Bar = mean ± SD，n=3. (*P<0.05, ***P<.001)

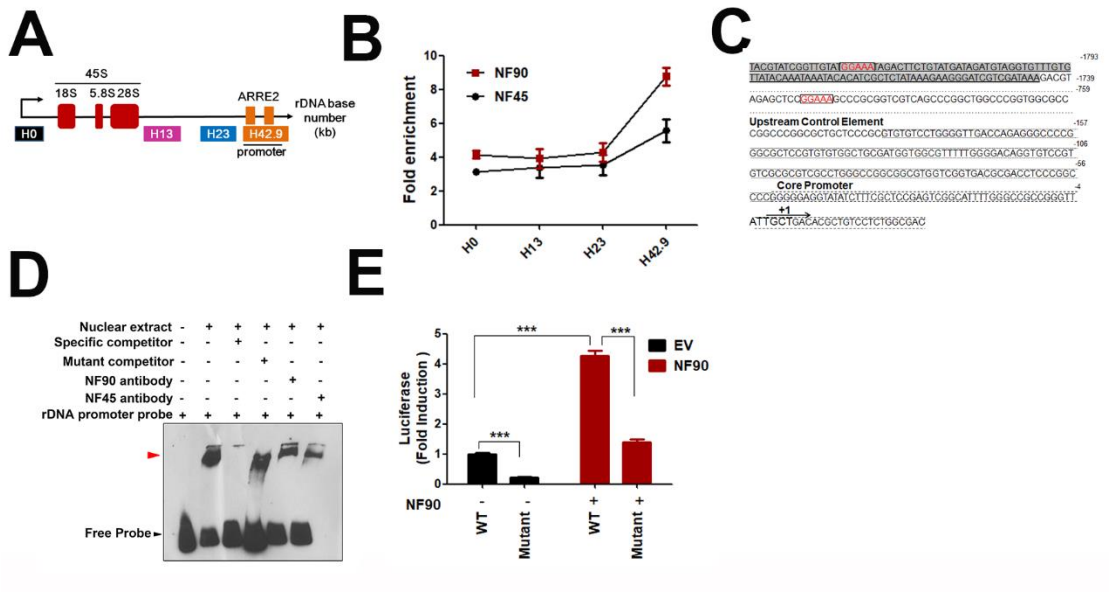


**Figure 2. NF45/NF90 preferentially binds to the promoter region of the rDNA gene loci by directly recognizing ARRE consensus sequences.** (A) Schematic illustration of a single human rDNA repeat and positions of the primers used for ChIP. (B) In Jurkat cells, a ChIP assay was performed with control IgG, NF45 NF90 antibodies, and then the precipitated DNA was analyzed using qPCR with the aforementioned primers. The relative rDNA fold-enrichment was normalized to control IgG treatment. (C) The human rDNA promoter region contains two putative NF90-binding sites (colored red). The grey box indicates the rDNA promoter probe in panel D. (D) EMSA data from nuclear extracts of HEK293 cells using the details described in Materials and Methods section. (E) The relative luciferase activity of HEK293T cells transfected with empty vector (EV) or Flag-NF90 (NF90) in combination with wild type (WT) or ARRE-mutated rDNA-Luc reporter plasmids (Mutant) for 24 h.

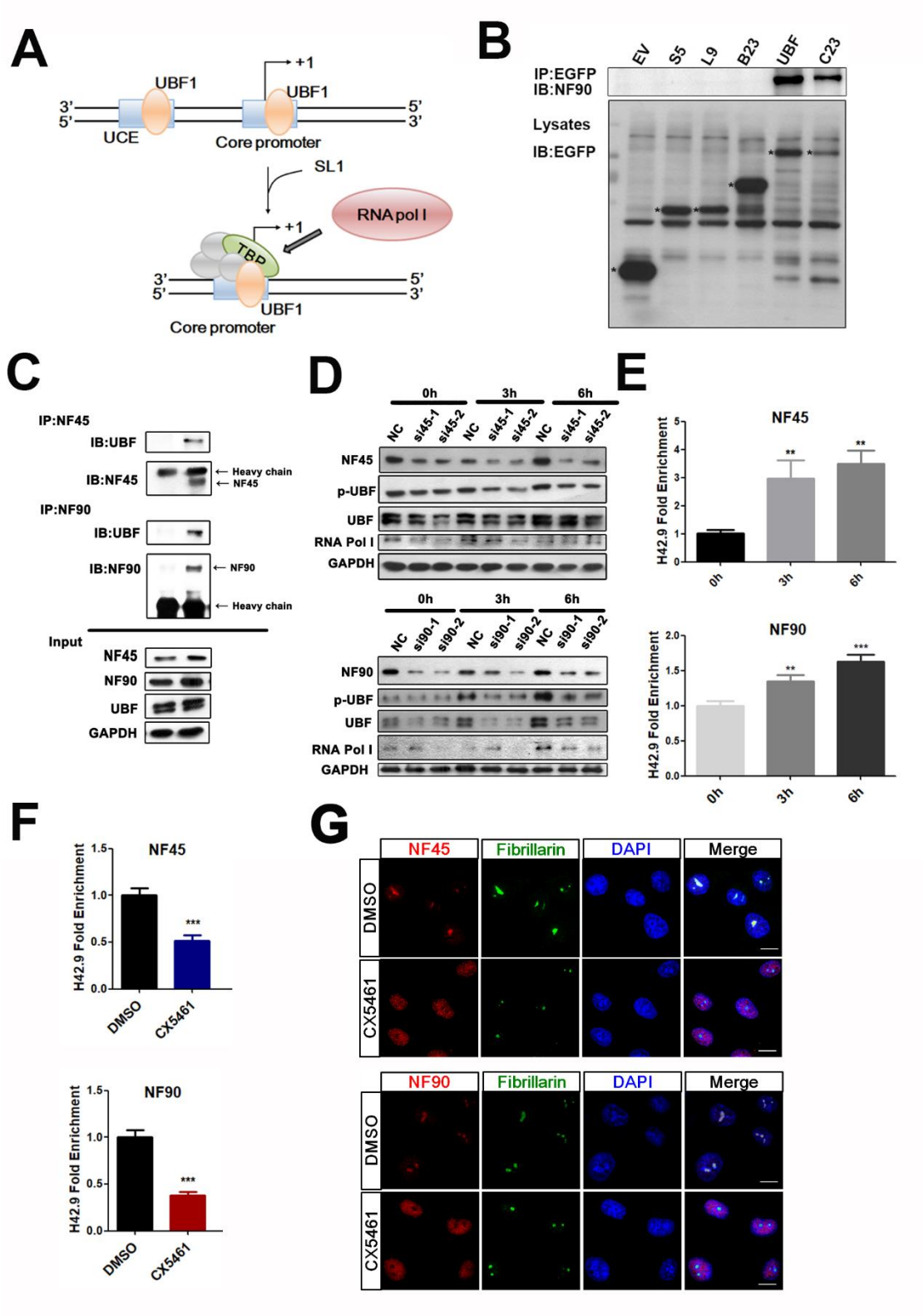


**Figure 3. NF45/NF90 affects rDNA transcription as a positive regulatory factor by recruiting and regulating UBF1 activity.** (A) The regulatory mechanism of the rDNA transcription. Firstly, the core promoter trans-acting element UBF1 binds to the rDNA promoter

to recruit SL1, then SL1 recruits Pol I for rDNA transcription. (B) Co-IP analysis of nucleolar proteins with NF45 and NF90 in HEK293 cells were transfected with EV, and the following plasmids: GFP-S5, GFP-L9, GFP-B23, GFP-UBF, GFP-C23. * for the target protein. (C) Co-IP analysis of UBF with NF45 and NF90 in HEK293 cells. (D) HEK293 cells were transfected with NF45-specfic siRNAs, NF90-specfic siRNAs, and then cells were stimulated in serum for 0, 3 and 6 h. Cell lysates were prepared at 48 h post-transfection to analyze NF45/NF90 levels by western blotting. (E) ChIP analysis was used to determinate the binding ability of NF45 and NF90 to rDNA promoters in Jurkat cells stimulated with serum for 0, 3 and 6 h. (F) ChIP analysis of NF45 and NF90 binding to the H42.9 loci in Jurkat cells with the treatment of CX5461 or DMSO for 2 h. (G) Confocal images of Jurkat cells treated with CX5461 for 2 h showing NF45 and NF90 colocalized with fibrillarin in nucleoli. Scale bar, 10 μm. In all panels, bar = mean ± SD，n=3.

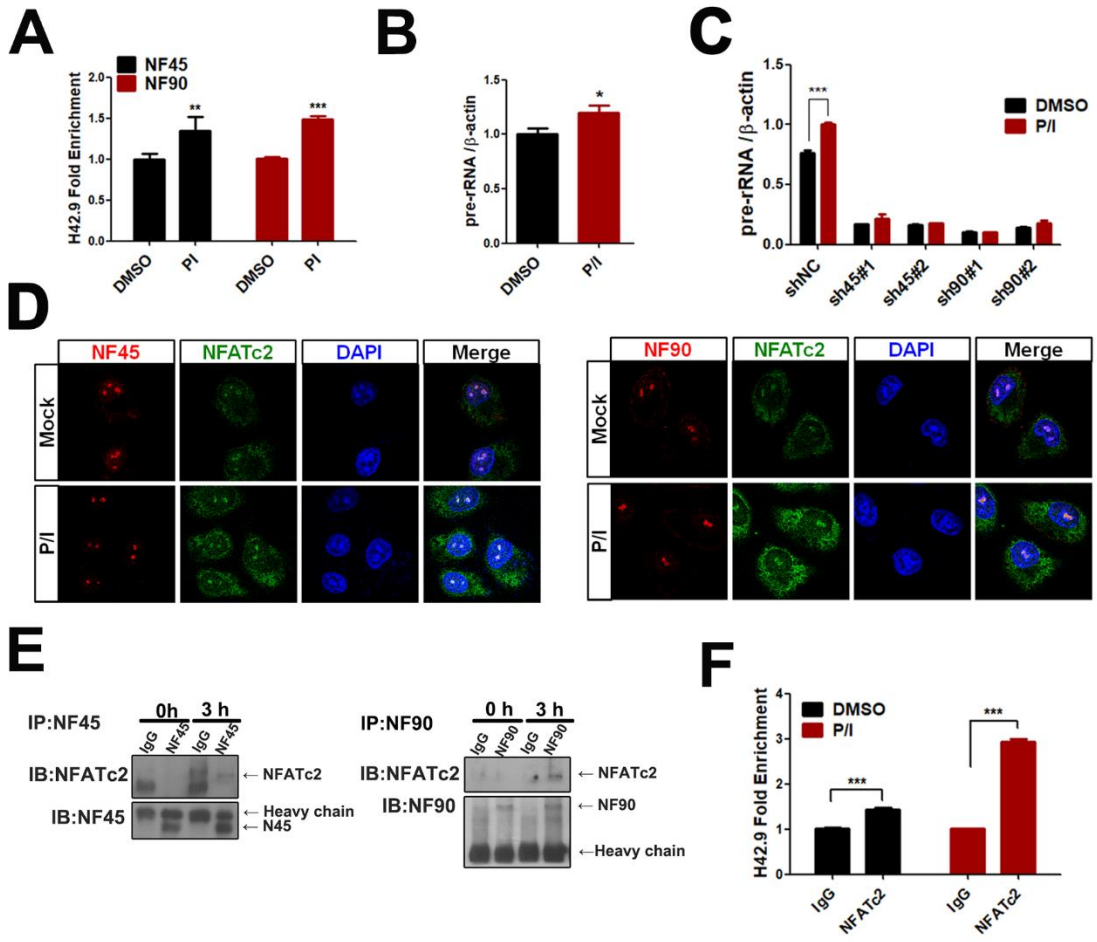


**Figure 4. NF45/NF90-mediated rDNA transcription contributes to T cell activation by interacting with NFATc2 in the nucleolus.** (A) ChIP analysis of NF45 and NF90 binding to the H42.9 loci in $CD3^+$ T cells stimulated with P/I for 6 h. (B) qPCR analysis of pre-rRNA in $CD3^+$ T cells treated with P/I for 6 h. (C) $CD3^+$ T cells were first silenced with negative shRNA (shNC), NF45 shRNAs (sh45) or NF45 shRNAs (sh90), and then treated with P/I to extract total RNA for qPCR analysis of pre-rRNA. (D) Confocal images of Jurkat cells to show NF45 (left panel) or NF90 (right panel) (green fluorescence) colocalized with NFATc2 (red fluorescence) in nucleoli. Scale bar, 10 μm. (E) Co-IP analysis of NFATc2 with NF45 and NF90 in Jurkat cells. (F) ChIP analysis of NFATc2 binding to the rDNA loci in CD3+ T cells stimulated with P/I (PMA/Ionomycin) for 6 h.

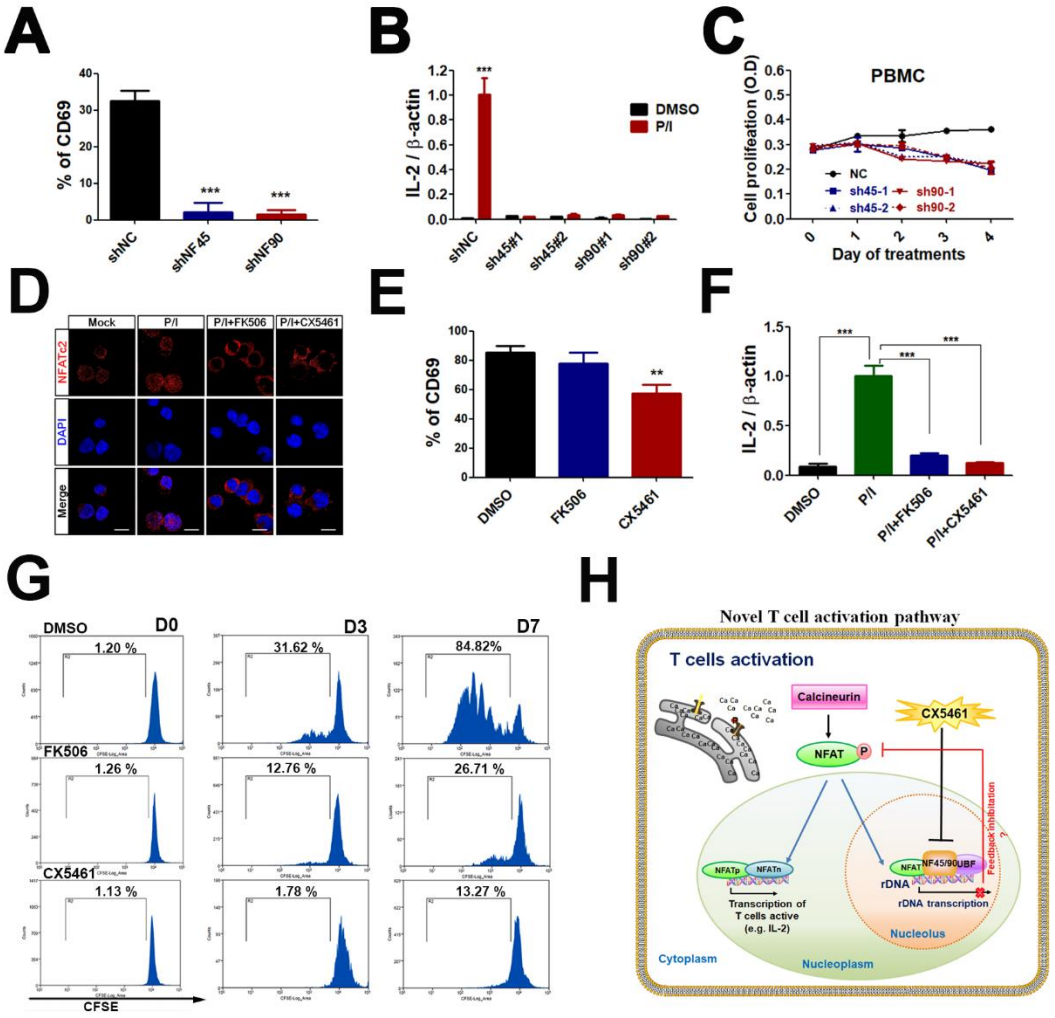


**Figure 5. NF45/NF90-mediated rDNA transcription is necessary for cell proliferation and activation.** (A) CD69 expression, an early marker of lymphocyte activation, in $CD3^+$ T cells upon stimulation with P/I for 6 h. (B) qPCR analysis of IL-2 mRNA expression from samples in panel E. (C) The proliferation of PBMC was monitored using a CCK-8 assay. (D) Confocal images to show the subcellular localization of NFATc2 in $CD3^+$ T cells treated with P/I and FK506 or CX5461. Scale bar, 10 μm. (E) Flow cytometry analysis of CD69 expression in P/I-stimulated $CD3^+$ T cells treated with or without FK506 or CX5461. (F) qPCR analysis of IL-2 mRNA expression in $CD3^+$ T cells with the indicated treatments. (G) Flow cytometry analysis of CFSE-labeled CD3+ T cells in the presence of DMSO, FK506 and CX5461 for 0, 3 and 7 d. (H) Schematic diagram: NF45/NF90-mediated rDNA transcription coordinates with NFAT signaling in regulating T cell activation. In all panels,

bar = mean ± SD，n=3, **P* < 0.05, ***P* < 0.01, ****P* < 0.001.

-

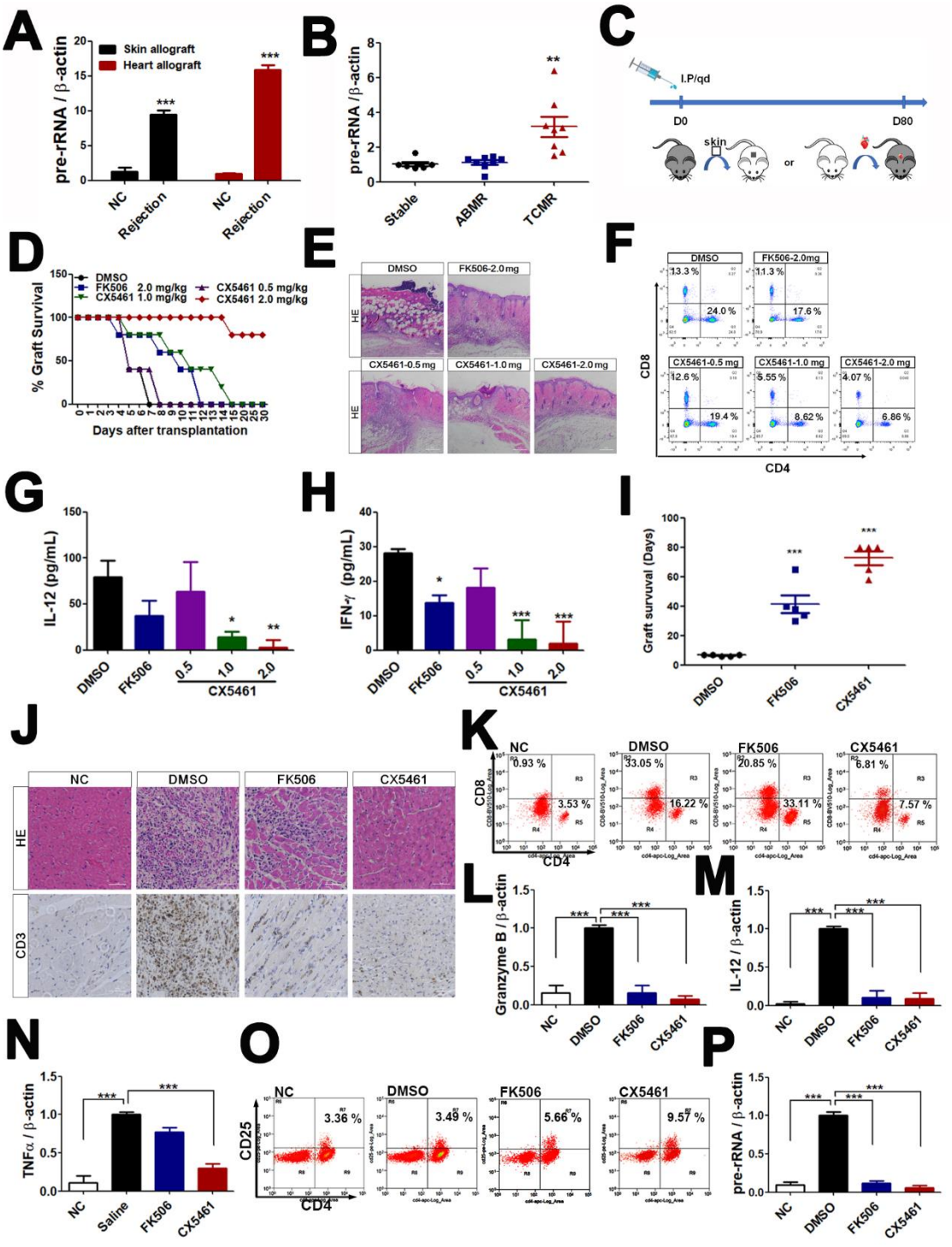


**Figure 6. CX5461 promotes graft survival in skin and cardiac allograft models.** (A) qPCR analysis of pre-rRNA expression from skin- and heart-transplanted mouse spleens. (B)

pre-rRNA expression levels of PBMC from renal transplantation patients. (Stable group, n=7. ABMR group, n=8. TCMR group, n=8). (C) Therapeutic scheme showing the daily administration of CX5461 or FK506 in skin- and cardiac-allografted mice until day 80. (D) Skin graft survival curve in mice treated with DMSO, 2.0 mg/kg FK506 or 0.5–2.0 mg/kg CX5461. At least five mice from each group were used in the experiments. (E) Representative images of HE staining of skin graft at seven days post transplantation. Scale bar = 50 μm. (F) FACS analysis of spleen T cells labeled with CD3, CD4 and CD8 antibodies. (G and H) ELISA analysis of IL-12 and IFN-γ levels in recipient mouse serum at four days post transplantation. (I) The survival time (days) of cardiac graft in mice treated with DMSO, 2.0 mg/kg FK506 or 2.0 mg/kg CX5461. At least five mice from each group were used in the experiments. (J) Representative images of HE and CD3-IHC staining of cardiac graft at seven days post transplantation. Scale bar = 100 μm. (K) FACS analysis of isolated mononuclear cells from transplanted heart labeled with CD3, CD4 and CD8 antibodies. (L-N) qPCR analysis of mRNA expression levels of granzyme B, IL-12 and TNF-α from heart-transplanted mouse spleens. (O) FACS analysis of isolated mononuclear cells from heart-transplanted mouse lymph nodes labeled with CD25 and CD4 antibodies. (P) qPCR analysis of pre-rRNA expression from transplanted mouse spleen. Bar = 50 μm, mean ± SEM，n=5. In all panels, ***$P < 0.001$.

## *Supporting Information*

### Supplementary Figure 1

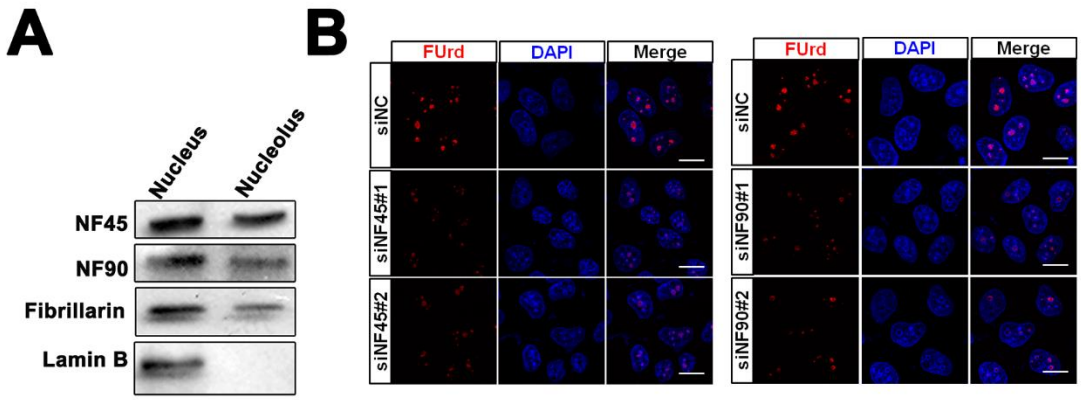


**Figure S1. NF45/NF90 is a nucleolar protein complex and positively regulates rDNA transcription** (related to Figure 1)**.** (A) HeLa cells were fractionated into cytoplasmic, nuclear, and nucleolar fractions, and protein extracts were analyzed using western blotting. Fibrillarin is a nucleolar marker; Lamin B is a nucleoplasm marker. (B) Confocal images of HeLa cells were silenced with negative siRNA (siNC), NF45 siRNAs (si45#1 or si45#2) or NF90 siRNAs (si90#1 or si90#2) for 48 h, and then pulsed with FUrd for another 15 min. in order to stain with an anti-BrdU (red). Scale bar, 10 μm.

**Supplementary Figure 2**

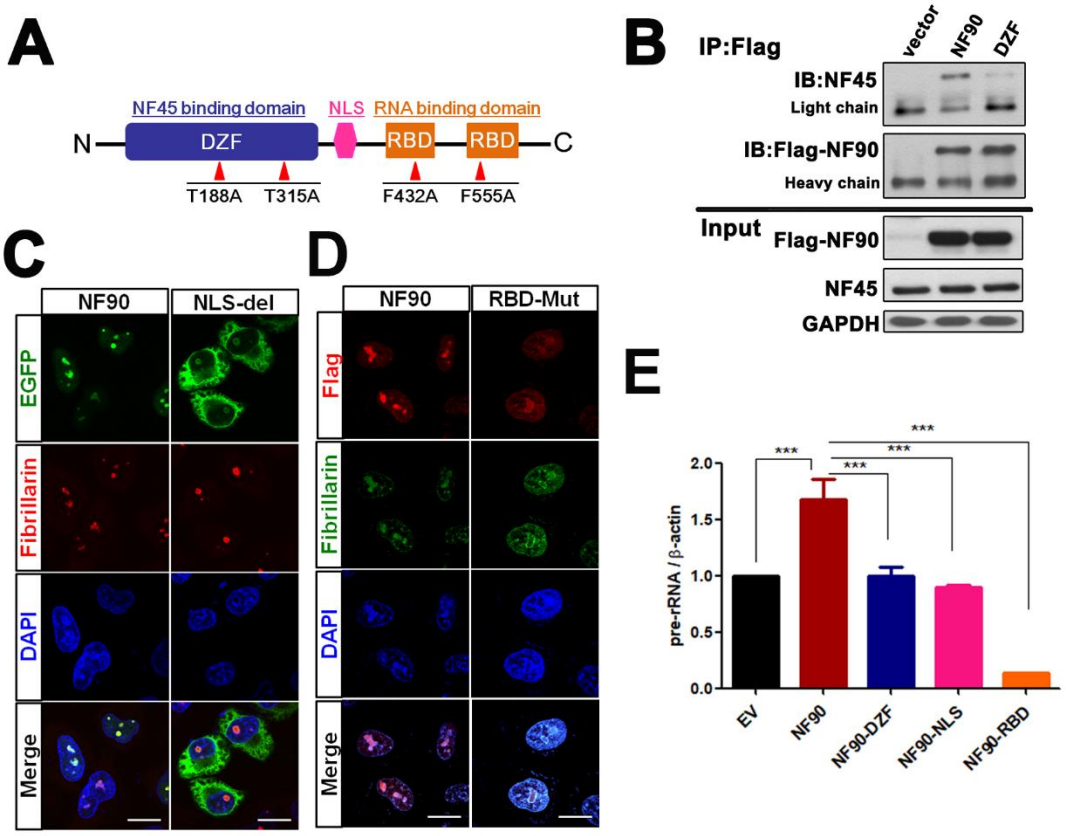


**Figure S2. The rDNA transcriptional regulation of NF45/NF90 requires it to act as a complex and locate in the nucleolus.** (related to Figure 1)**.** (A) Schematic diagram showing the domains of NF90 and its mutations (point mutations in DZF and RBD domains or NLS deleted mutations). (B) Co-IP analysis of NF45 with wild-type NF90 or DZF-mutated NF90. (C) Confocal images of HEK293 cells transfected with NF90-EGFP or NF90-NLS-EGFP plasmid (fibrillarin is a nucleolar marker). (D) Confocal images of HEK293 cells transfected with NF90-Flag or NF90-RBD-Flag plasmid. Scale bar, 10 μm. (E) HEK293 cells were transfected with an NF90-flag vector or mutated vectors (DZF, NLS, or RBD) for 24 h, and then the total RNA was extracted from cells for qPCR analysis of pre-rRNA. Bar = mean ± SD，n=3. (*P<0.05, ***P<.001)

**Supplementary Figure 3**

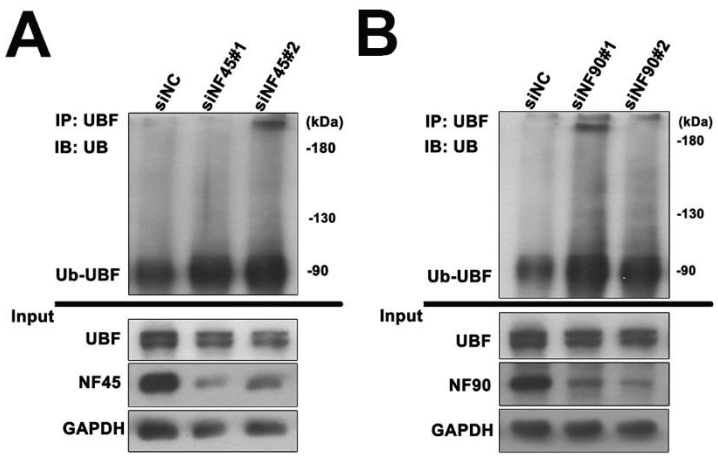


**Figure S3. NF45 and NF90 knockdown increased UBF ubiquitination** (related to Figure 3)**.** (A and B) Co-IP analysis of Ubiquitin with NF45 (A) and NF90 (B) in HEK293 cells transfected with NF45-specfic siRNAs (siNF45#1 and siNF45#2) or NF90-specfic siRNAs (siNF90#1 and siNF90#2).

**Supplementary Figure 4**

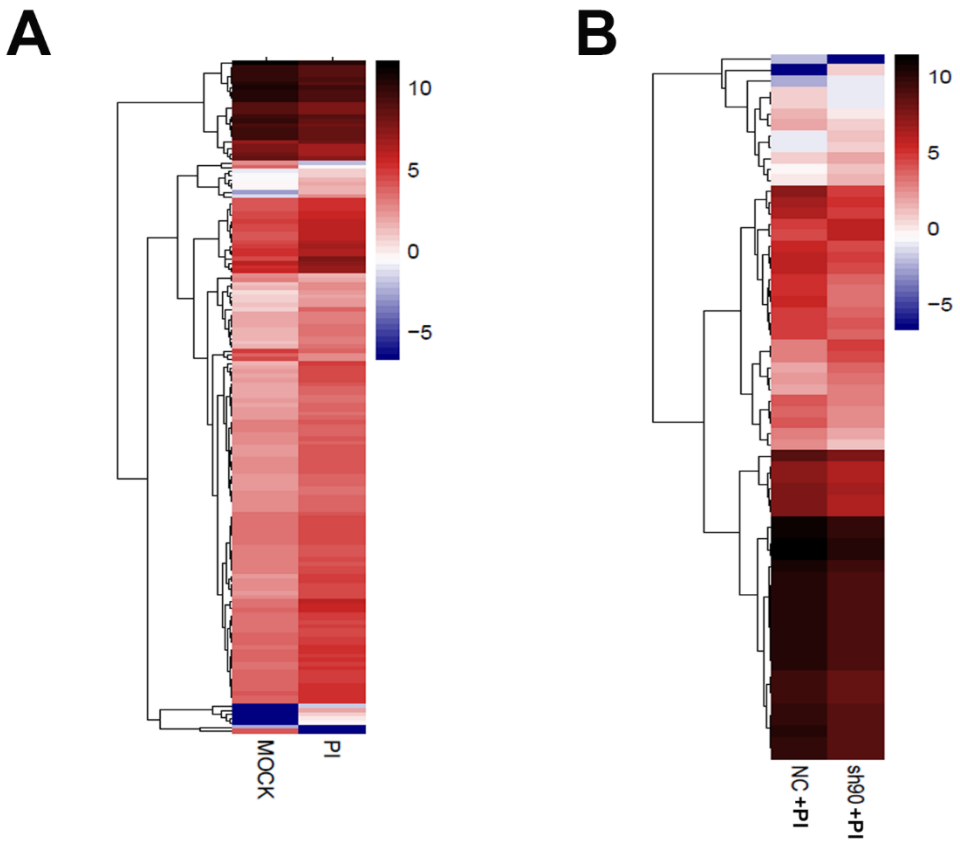


**Figure S4. RNA sequencing reveals genes related to ribosome biogenesis were differentially expressed in NF90-knockdown T cells upon P/I treatment** (related to Figure 4). (A) Heatmaps showing the expression data of the 161 differentially expressed ribosome biogenesis-related genes between P/I vs Mock in T cells. (B) Heatmaps showing the expression data of the 64 differentially expressed ribosome biogenesis-related genes between sh90 vs NC in T cells upon P/I treatment.

**Supplementary Figure 5**

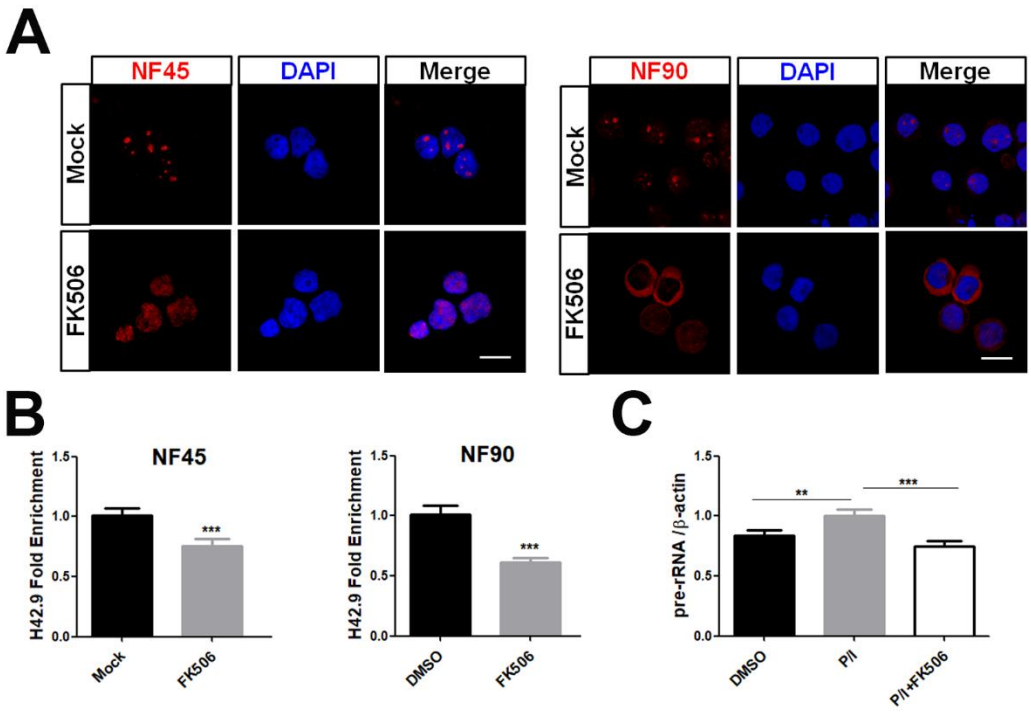


**Figure S5. Calcineurin inhibitors affect the subcellular localization of NF45/NF90 and rDNA transcription in T cells** (related to Figure 4)**.** (A) Confocal images show the localization of NF45 (left panel) or NF90 (right panel) in P/I-stimulated $CD3^+$ T cells treated with or without FK506. Scale bar = 10 μm. (B) The binding of NF45 and NF90 to the H42.9 loci in P/I-stimulated $CD3^+$ T cells treated with or without FK506. (C) qPCR analysis of pre-rRNA in $CD3^+$ cells treated with P/I and a combination of P/I and FK506.

**Supplementary Figure 6**

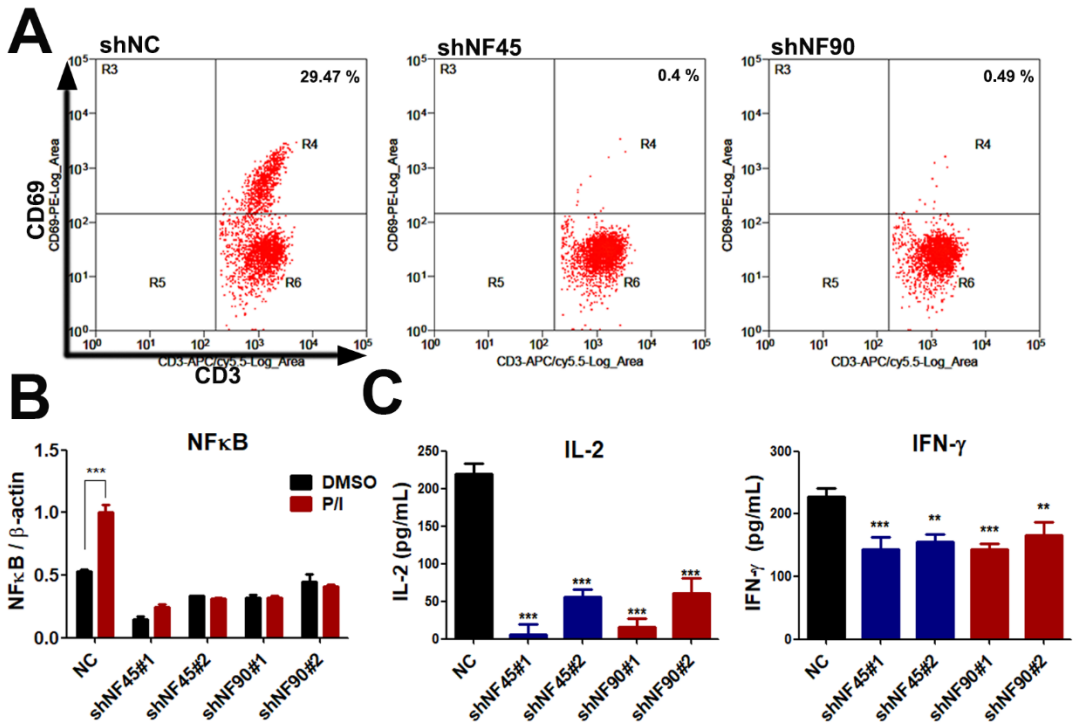


**Figure S6. NF45/NF90 knockdown inhibits T cell activation** (related to Figure 5)**.** (A) Flow cytometry analysis of CD69 expression in shNC, shNF45 and shNF90-CD3$^+$ T cells stimulated with P/I for 6 h. (B) qPCR analysis of NF-κB in shNC, shNF45 or shNF90-CD3$^+$ T cells stimulated with P/I for 6 h. (C) ELISA of IL-2 and IFN-γ levels in shNC, shNF45 or shNF90-PBMC cells stimulated with P/I for 6 h. Results are expressed as mean ± SD for three replicates.

**Supplementary Figure 7**

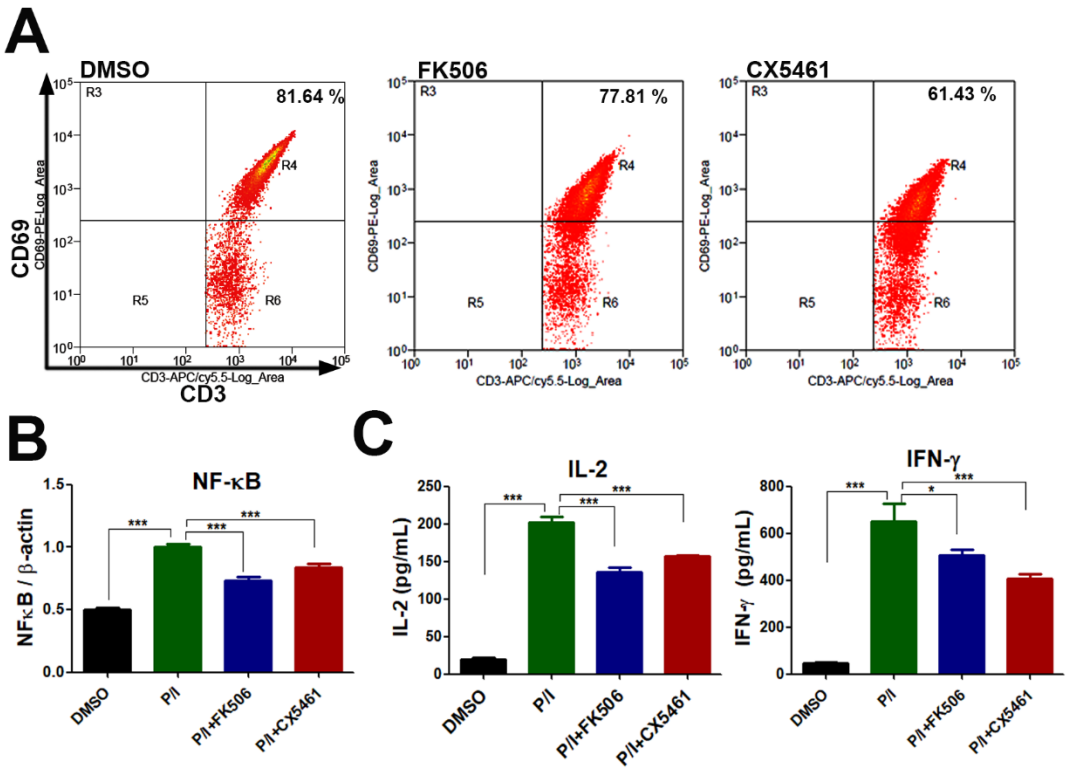


**Figure S7. The Pol I inhibitor CX5461 inhibits T cell activation** (related to Figure 5)**.** (A) Flow cytometry analysis of CD69 expression in P/I-stimulated $CD3^+$ T cells treated with FK506 or CX5461. (B) qPCR analysis of NF-κB in P/I-stimulated $CD3^+$ T cells treated with FK506 or CX5461. (C) ELISA analysis of IL-2 and IFN-γ levels in P/I-stimulated PBMC treated with FK506 or CX5461. Results are expressed as mean ± SD for three replicates.

**Supplementary Figure 8**

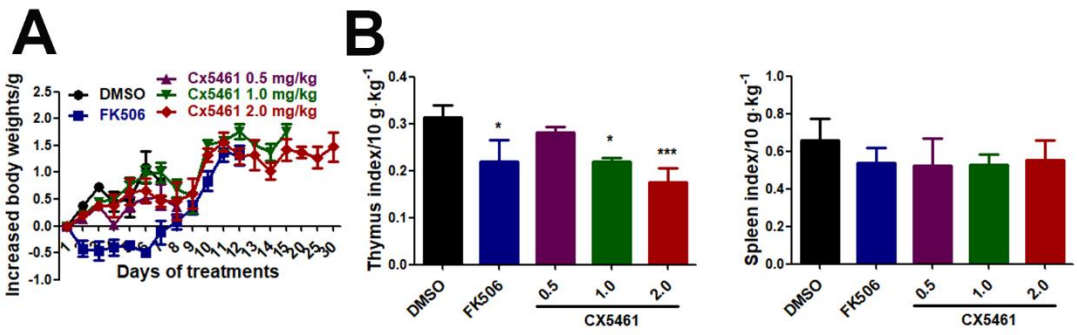


**Figure S8. The effects of CX5461 on the body weights, and both spleen and thymus weights of skin-graft mice** (related to Figure 5)**.** (A) Plots of the body weights of skin-graft mice after injecting with DMSO, FK506 or different doses of CX5461. (B) The thymuses and spleens of each group were weighed at the end point of the study.

**Supplementary Figure 9**

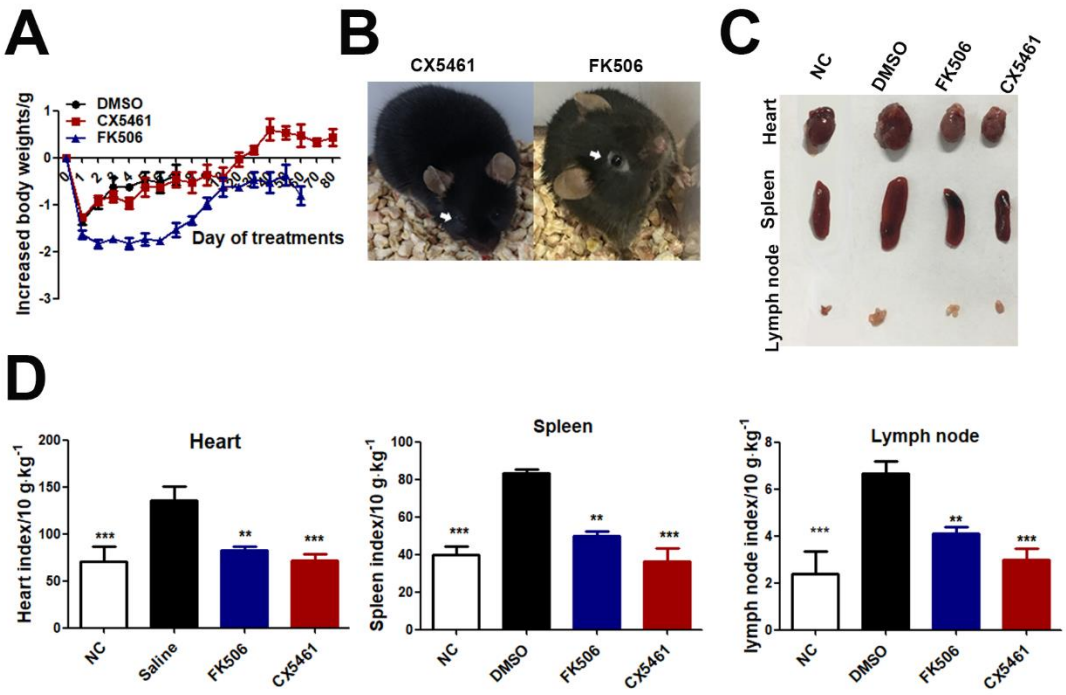


**Figure S9. The effects of CX5461 on the body weights, hair loss, and spleen and thymus weights of heart-transplant mice** (related to Figure 6)**.** (A) Plots of body weights of heart-transplant mice after injecting with DMSO, FK506 or CX5461. (B) Images highlighting the hair loss of heart-transplant mice after injecting with FK506 or CX5461 at Day 7. Images (C) and weights (D) of the viscera of heart-grafts, spleens and lymph nodes of each group at the end point of the study.

**Supplementary Figure 10**

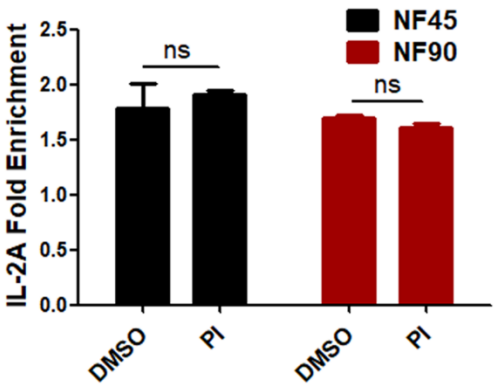


**Figure S10. NF45 and NF90 binding to IL-2 in activated T cells** (related to Figure 4)**.** The binding ability of NF45 or NF90 to the IL-2 loci detected by a ChIP assay in $CD3^+$ cells stimulated with or without of P/I for 6 h.